Family of Controllers for Attitude Synchronization on the Sphere ⋆

Pedro O. Pereira [a] and Dimos V. Dimarogonas [a]

[a] *ACCESS Linnaeus Center and KTH Centre for Automomous Systems, School of Electrical Engineering, KTH Royal Institute of Technology, Stockholm, Sweden.*

Abstract

In this paper we study a family of controllers that guarantees attitude synchronization for a network of agents in the unit sphere domain, i.e., $\mathcal{S}^2$. We propose distributed continuous controllers for elements whose dynamics are controllable, i.e., control with torque as command, and which can be implemented by each individual agent without the need of a common global orientation frame among the network, i.e., it requires only local information that can be measured by each individual agent from its own orientation frame. The controllers are constructed as functions of distance functions in $\mathcal{S}^2$, and we provide conditions on those distance functions that guarantee that *i)* a synchronized network of agents is locally asymptotically stable for an arbitrary connected network graph; *ii)* a synchronized network is asymptotically achieved for almost all initial conditions in a tree network graph. When performing synchronization along a principal axis, we propose controllers that do not require full torque, but rather torque orthogonal to that principal axis; while for synchronization along other axes, the proposed controllers require full torque. We also study the equilibria configurations that come with specific types of network graphs. The proposed strategies can be used in attitude synchronization of swarms of under actuated rigid bodies, such as satellites.

1 Introduction

Decentralized control in a multi-agent environment has been a topic of active research for the last decade, with applications in large scale robotic systems. Attitude synchronization in satellite formations is one of those applications [Lawton and Beard, 2002], where the control goal is to guarantee that a network of fully actuated rigid bodies acquires a common attitude. Coordination of underwater vehicles in ocean exploration missions can also be casted as an attitude synchronization problem [Leonard et al., 2007].

In the literature of attitude synchronization, different solutions for consensus in the special orthogonal group are found [Bondhus et al., 2005, Cai and Huang, 2014, Dimarogonas et al., 2009, Krogstad and Gravdahl, 2006, Lawton and Beard, 2002, Nair and Leonard, 2007, Sarlette et al., 2009, Song et al., 2015, Thunberg et al., 2014], which focus on *complete* attitude synchronization. In this paper, we focus on *incomplete* attitude synchronization, which has not received the same attention: in this scenario, each rigid body has a main direction and the global objective is to guarantee alignment of all rigid bodies' main directions; the space orthogonal to each main direction can be left free of actuation or controlled to accomplish some other goals. Complete attitude synchronization requires more measurements when compared to incomplete attitude synchronization, and it might be the case that a rigid body is not fully actuated but rather only actuated in the space orthogonal to a specific direction, in which case incomplete attitude synchronization is still feasible. *Incomplete* attitude synchronization is also denoted synchronization on the sphere in [Dörfler and Bullo, 2014, Li and Spong, 2014, Moshtagh and Jadbabaie, 2007, Olfati-Saber, 2006, Paley, 2009, Sarlette et al., 2008], where the focus has been on kinematic or point mass dynamic agents, i.e., dynamical agents without moment of inertia.

In [Dimarogonas et al., 2009], attitude control in a leader-follower network of rigid bodies has been studied, with the special orthogonal group being parametrized with Modified Rodrigues Parameters. The proposed solution guarantees attitude synchronization for connected graphs, but it requires all rigid bodies to be aware of a common and global orientation frame. In [Bondhus et al., 2005, Krogstad and Gravdahl, 2006], a controller for a single-leader single-follower network is proposed that guarantees global attitude synchronization at the cost of introducing a discontinuity in the control laws. In [Cai and Huang, 2014], attitude synchronization in a

⋆ This work was supported from the EU H2020 Research and Innovation Programme under GA No.644128 (AEROWORKS), the Swedish Research Council (VR), the Swedish Foundation for Strategic Research (SSF) and the KAW Foundation. Email addresses: `{ppereira, dimos}@kth.se`.

Email addresses: `ppereira@kth.se` (Pedro O. Pereira), `dimos@kth.se` (Dimos V. Dimarogonas).

leader-follower network is accomplished by designing a non-linear distributed observer for the leader. In [Chung et al., 2009, 2013], a combination of a tracking input and a synchronization input is used; the tracking input adds robustness if connectivity is lost and it is designed in the spirit of leader-following, where the leader is a virtual one and it encapsulates a desired trajectory; however, this strategy requires all agents to be aware of a common and global reference frame. In another line of work, in [Nair and Leonard, 2007, Sarlette et al., 2009], attitude synchronization is accomplished without the need of a common orientation frame among agents. Additionally, in [Sarlette et al., 2009], a controller for switching and directed network topologies is proposed, and local stability of consensus in connected graphs is guaranteed, provided that the control gain is sufficiently high. In [Lawton and Beard, 2002], attitude synchronization is accomplished with controllers based on behavior based approaches and for a bidirectional ring topology. The special orthogonal group is parametrized with quaternions, and the proposed strategy also requires a common attitude frame among agents. In [Mayhew et al., 2012], a quaternion based controller is proposed that guarantees a synchronized network of rigid bodies is a global equilibrium configuration, provided that the network graph is acyclic. This comes at the cost of having to design discontinuous (hybrid) controllers. A discrete time protocol for complete synchronization of kinematic agents is found in [Tron et al., 2012]. The authors introduce the notion of *reshaping function*, and a similar concept is presented in this manuscript. The protocol provides almost global convergence to a synchronized configuration, which relies on proving that all other equilibria configurations, apart from the equilibria configuration where agents are synchronized, are unstable. In [Thunberg et al., 2014], controllers for complete attitude synchronization and for switching topologies are proposed, but this is accomplished at the kinematic level, i.e., by controlling the agents' angular velocity (rather than their torque). This work is extended in [Song et al., 2015] by providing controllers at the torque level, and similarly to [Lawton and Beard, 2002], stability properties rely of high gain controllers.

In [Moshtagh and Jadbabaie, 2007, Olfati-Saber, 2006], incomplete synchronization of kinematic agents on the sphere is studied, with a constant edge weight function for all edges. In particular, in [Moshtagh and Jadbabaie, 2007], incomplete synchronization is used for accomplishing a flocking behavior, where a group of agents moves in a common direction. In [Paley, 2009], dynamic agents, which move at constant speed on a sphere, are controlled by a state feedback control law that steers their velocity vector so as to force the agents to attain a collective circular motion; since the agents are mass points, the effect of the moment of inertia is not studied. In [Li and Spong, 2014], dynamic point mass agents, constrained to move on a sphere, are controlled to form patterns on the sphere, by constructing attractive and repelling forces; in the absence of repelling forces, synchronization is achieved. Also, the closed-loop dynamics of these agents are invariant to rotations, or symmetry preserving, as those in [Moshtagh and Jadbabaie, 2007, Olfati-Saber, 2006], in the sense that two trajectories, whose initial condition – composed of position and velocity – differs only on a rotation, are the same at each time instant apart from the previous rotation. In our framework this property does not hold, since our dynamic agents have a moment of inertia, unlike the agents in [Li and Spong, 2014, Moshtagh and Jadbabaie, 2007, Olfati-Saber, 2006], which is another novelty of the paper in hand.

We propose a distributed control strategy for synchronization of elements in the unit sphere domain. The controllers for accomplishing synchronization are constructed as functions of distance functions (or *reshaping functions* as denoted in [Tron et al., 2012]), and, in order to exploit results from graph theory, we impose a condition on those distance functions that will restrict them to be invariant to rotations of their arguments. As a consequence, the proposed controllers can be implemented by each agent without the need of a common orientation frame. We restrict the proposed controllers to be continuous, which means that a synchronized network of agents cannot be a global equilibrium configuration, since $\mathcal{S}^2$ is a non-contractible set [Liberzon, 2003]. Our main contributions lie in proposing for the first time a controller that does not require full torque when performing synchronization along a principal axis, but rather torque orthogonal to that axis; in finding conditions on the distance functions that guarantee that a synchronized network is locally asymptotically stable for arbitrary connected network graphs, and that guarantee that a synchronized network is achieved for almost all initial conditions in a tree graph; in providing explicit domains of attraction for the network to converge to a synchronized network; and in characterizing the equilibria configurations for some general, yet specific, types of network graphs. A preliminary version of this work was submitted to the 2015 IEEE Conference on Decision and Control [Pereira and Dimarogonas, 2015]. With respect to this preliminary version, this paper presents significantly more details on the derivation of the main theorems and provides additional results. In particular, the concept of cone has been modified, with a clearer intuitive interpretation; the proof for the proposition that supports the result on local stability of the synchronized network has been simplified; further details on the condition imposed on the distance functions are provided; additional examples on possible distance functions, and their properties, are presented; and supplementary simulations are provided which further illustrate the theoretical results. The remainder of this paper is structured as follows. In Section 3, the problem statement is described; in Section 4, the proposed solution is presented; in Sections 5 and 6, convergence to a synchronized network is discussed for tree and arbitrary graphs, respectively; and, in Section 7, simulations are presented that illustrate the theoretical results.

2 Notation

$\mathbf{0}_n \in \mathbb{R}^n$ and $\mathbf{1}_n \in \mathbb{R}^n$ denote the zero column vector and the column vector with all components equal to 1, respectively; when the subscript n is omitted, the dimension n is assumed to be of appropriate size. $\mathrm{I}_n \in \mathbb{R}^{n\times n}$ stands for the identity matrix, and we omit its subscript when $n = 3$. The matrix $\mathcal{S}(\cdot) \in \mathbb{R}^{3\times 3}$ is a skew-symmetric matrix and it satisfies $\mathcal{S}(\mathbf{a})\ \mathbf{b} = \mathbf{a}\times\mathbf{b}$, for any $\mathbf{a}, \mathbf{b} \in \mathbb{R}^3$. The map $\Pi : \{\mathbf{x} \in \mathbb{R}^3 : \mathbf{x}^T\mathbf{x} = 1\} \mapsto \mathbb{R}^{3\times 3}$, defined as $\Pi(\mathbf{x}) = \mathrm{I} - \mathbf{x}\mathbf{x}^T$, yields a matrix that represents the orthogonal projection operator onto the subspace perpendicular to $\mathbf{x}$. We denote the Kronecker product between $A \in \mathbb{R}^{m\times n}$ and $B \in \mathbb{R}^{s\times t}$ by $A \otimes B \in \mathbb{R}^{m\,s\times n\,t}$. Given $A_1, \cdots, A_n \in \mathbb{R}^{m\times m}$, for some $n, m \in \mathbb{N}$, we denote $A = A_1 \oplus \cdots \oplus A_n \in \mathbb{R}^{nm\times nm}$ (direct sum of matrices) as the block diagonal matrix with block diagonal entries A_1 to A_n. Given $\mathbf{a}, \mathbf{b} \in \mathbb{R}^n$, $\mathbf{a} = \pm\mathbf{b} \Leftrightarrow \mathbf{a} = \mathbf{b} \vee \mathbf{a} = -\mathbf{b}$; additionally, we say $\mathbf{a} \neq \mathbf{0}$ and $\mathbf{b} \neq \mathbf{0}$ have the same direction if there exists $\lambda \in \mathbb{R}$ such that $\mathbf{b} = \lambda\mathbf{a}$. We say a function $f : \Omega_1 \mapsto \Omega_2$ is of class $\mathcal{C}^n$, or equivalently $f \in \mathcal{C}^n(\Omega_1, \Omega_2)$, if its first $n+1$ derivatives (i.e., $f^{(0)}$, $f^{(1)}$, $\cdots$, $f^{(n)}$) exist and are continuous on Ω_1. Finally, given a set $\mathcal{H}$, we use the notation $|\mathcal{H}|$ for the cardinality of $\mathcal{H}$.

3 Problem Statement

We consider a group of N agents, indexed by the set $\mathcal{N} = \{1, \cdots, N\}$, operating in the unit sphere domain, i.e., in $\mathcal{S}^2 = \{\mathbf{x} \in \mathbb{R}^3 : \mathbf{x}^T\mathbf{x} = 1\}$. The agents' network is modeled as an undirected static graph, $\mathcal{G} = \{\mathcal{N}, \mathcal{E}\}$, with $\mathcal{N}$ as the vertices' set indexed by the team members, and $\mathcal{E}$ as the edges' set. For every pair of agents $(i, j) \in \mathcal{E}$, that are *aware of* and can measure each other's relative attitude, we say that agent j is a neighbor of agent i, and vice-versa; also, we denote $\mathcal{N}_i \subset \mathcal{N}$ as the neighbor set of agent i.

Each agent i has its own orientation frame (w.r.t. an unknown inertial orientation frame), represented by $\mathcal{R}_i \in \mathcal{SO}(3)$. Let the unit vector $\mathbf{n}_i \in \mathcal{S}^2$ be a direction along agent's i orientation, i.e., $\mathbf{n}_i = \mathcal{R}_i\bar{\mathbf{n}}_i$, where $\bar{\mathbf{n}}_i \in \mathcal{S}^2$ is a constant unit vector, specified in the agent's i body orientation frame, and known by agent i and its neighbors. In this paper, the goal of attitude synchronization is not that all agents share the same *complete* orientation, i.e., that $\mathcal{R}_1 = \cdots = \mathcal{R}_N$, but rather that all agents share the same orientation along a specific direction, i.e., that $\mathbf{n}_1 = \cdots = \mathbf{n}_N \Leftrightarrow \mathcal{R}_1\bar{\mathbf{n}}_1 = \cdots = \mathcal{R}_N\bar{\mathbf{n}}_N$. For example, in a group of N satellites that must align their principal axis associated to the smallest moment of inertia, it follows that, for each $i \in \mathcal{N}$, $\bar{\mathbf{n}}_i \in \mathcal{S}^2 : \exists\lambda_i > 0 : J_i\bar{\mathbf{n}}_i = \lambda_i\bar{\mathbf{n}}_i$ with J_i as the satellite's moment of inertia and with λ_i as the smallest eigenvalue of J_i; and that the desired synchronized network of satellites satisfies $\mathcal{R}_1\bar{\mathbf{n}}_1 = \cdots = \mathcal{R}_N\bar{\mathbf{n}}_N$. Figure 1 illustrates the concept of incomplete synchronization. Notice that agent i is not aware of $\mathbf{n}_i$, since this is specified w.r.t. an unknown inertial orientation frame; instead, agent i is aware of its own direction $\bar{\mathbf{n}}_i$ – fixed in its own orientation frame – and the projection of its neighbors directions onto its own orientation frame.

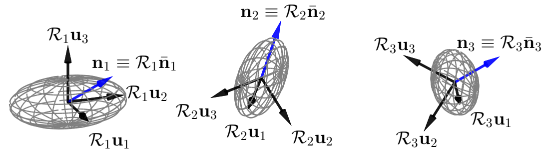

Fig. 1. Rigid bodies 1 and 3 are synchronized with each other, but not with rigid body 2. In incomplete synchronization, n rigid bodies, indexed by $i = \{1, \cdots, n\}$, synchronize the unit vectors $\mathbf{n}_i = \mathcal{R}_i\bar{\mathbf{n}}_i$, where $\bar{\mathbf{n}}_i$ is fixed in rigid body i. In this figure, $\bar{\mathbf{n}}_1 = -\bar{\mathbf{n}}_2 = -\bar{\mathbf{n}}_3 = \frac{1}{\sqrt{3}}[1\ 1\ 1]^T$ ($\mathbf{u}_1$,$\mathbf{u}_2$ and $\mathbf{u}_3$ stand for the canonical basis vectors of $\mathbb{R}^3$).

Consider then any agent $i \in \mathcal{N}$, with rotation matrix $\mathcal{R}_i : \mathbb{R}_{\geq 0} \mapsto \mathcal{SO}(3)$, unit vector $\mathbf{n}_i : \mathbb{R}_{\geq 0} \mapsto \mathcal{S}^2$ where $\mathbf{n}_i(\cdot) = \mathcal{R}_i(\cdot)\bar{\mathbf{n}}_i$, body-framed angular velocity $\boldsymbol{\omega}_i : \mathbb{R}_{\geq 0} \mapsto \mathbb{R}^3$, moment of inertia $J_i \in \mathbb{R}^{3\times 3}$ ($J_i > 0$), and body frame torque $\mathbf{T}_i : \mathbb{R}_{\geq 0} \mapsto \mathbb{R}^3$. The rotation matrix $\mathcal{R}_i : \mathbb{R}_{\geq 0} \mapsto \mathcal{SO}(3)$ evolves according to

$$\dot{\mathcal{R}}_i(t) = \mathbf{f}_{\mathcal{R}}(\mathcal{R}_i(t), \boldsymbol{\omega}_i(t)), \tag{3.1}$$

where $\mathbf{f}_{\mathcal{R}} : \mathcal{SO}(3) \times \mathbb{R}^3 \mapsto \mathbb{R}^{3\times 3}$ is defined as $\mathbf{f}_{\mathcal{R}}(\mathcal{R}, \boldsymbol{\omega}) = \mathcal{R}\mathcal{S}(\boldsymbol{\omega})$; while each unit vector $\mathbf{n}_i : \mathbb{R}_{\geq 0} \mapsto \mathcal{S}^2$ evolves according to $\dot{\mathbf{n}}_i(t) = \mathbf{f}_{\mathbf{n}_i}(t, \mathbf{n}_i(t), \boldsymbol{\omega}_i(t))$, where $\mathbf{f}_{\mathbf{n}_i} : \mathbb{R}_{\geq 0} \times \mathcal{S}^2 \times \mathbb{R}^3 \mapsto \mathbb{R}^3$ is defined as $\mathbf{f}_{\mathbf{n}_i}(t, \mathbf{n}, \boldsymbol{\omega}) = \mathcal{S}(\mathcal{R}_i(t)\boldsymbol{\omega})\,\mathbf{n}$. The previous result follows from the fact that $\mathbf{n}_i(\cdot) = \mathcal{R}_i(\cdot)\bar{\mathbf{n}}_i$ for some constant $\bar{\mathbf{n}}_i \in \mathcal{S}^2$, and therefore $\dot{\mathcal{R}}_i(t)\bar{\mathbf{n}}_i = \mathcal{S}(\mathcal{R}_i(t)\boldsymbol{\omega}_i(t))\,\mathcal{R}_i(t)\bar{\mathbf{n}}_i \Rightarrow \dot{\mathbf{n}}_i(t) = \mathcal{S}(\mathcal{R}_i(t)\boldsymbol{\omega}_i(t))\,\mathbf{n}_i(t)$. Finally, the body-framed angular velocity $\boldsymbol{\omega}_i : \mathbb{R}_{\geq 0} \mapsto \mathbb{R}^3$ evolves according to the dynamics

$$\dot{\boldsymbol{\omega}}_i(t) = J_i^{-1}\left(-\mathcal{S}(\boldsymbol{\omega}_i(t))\,J_i\boldsymbol{\omega}_i(t) + \mathbf{T}_i(t)\right), \tag{3.2}$$

and therefore $\dot{\boldsymbol{\omega}}_i(t) = \mathbf{f}_{\boldsymbol{\omega}_i}(\boldsymbol{\omega}_i(t), \mathbf{T}_i(t))$, where $\mathbf{f}_{\boldsymbol{\omega}_i} : \mathbb{R}^3 \times \mathbb{R}^3 \mapsto \mathbb{R}^3$ is defined as

$$\mathbf{f}_{\boldsymbol{\omega}_i}(\boldsymbol{\omega}, \mathbf{T}) = J_i^{-1}\left(-\mathcal{S}(\boldsymbol{\omega})\,J_i\boldsymbol{\omega} + \mathbf{T}\right). \tag{3.3}$$

Definition 3.1 Two unit vectors $(\mathbf{n}_1, \mathbf{n}_2) \in (\mathcal{S}^2)^2$ are diametrically opposed if $\mathbf{n}_1^T\mathbf{n}_2 = -1$, and synchronized if $\mathbf{n}_1^T\mathbf{n}_2 = 1$. A group of unit vectors $(\mathbf{n}_1, \cdots, \mathbf{n}_N) \in (\mathcal{S}^2)^N$ is synchronized if $\mathbf{n}_i^T\mathbf{n}_j = 1$ for all $i, j \in \{1, \cdots, N\}$.

Problem 3.1 Given a group of rotation matrices $(\mathcal{R}_1, \cdots, \mathcal{R}_N) : \mathbb{R}_{\geq 0} \mapsto \mathcal{SO}(3)^N$, with angular velocities $(\boldsymbol{\omega}_1, \cdots, \boldsymbol{\omega}_N) : \mathbb{R}_{\geq 0} \mapsto \mathbb{R}^3$ and moments of inertia $J_1, \cdots, J_N$ satisfying (3.1) and (3.2), design distributed control laws for the torques $\{\mathbf{T}_i : \mathbb{R}_{\geq 0} \mapsto \mathbb{R}^3\}_{i\in\mathcal{N}}$, in the absence of a common inertial orientation frame, that guarantee that the group of unit vectors $(\mathbf{n}_1, \cdots, \mathbf{n}_N) : \mathbb{R}_{\geq 0} \mapsto (\mathcal{S}^2)^N$ is asymptotically synchronized.

For the purposes of analysis, we consider the state $\mathbf{x} := (\mathbf{n}, \boldsymbol{\omega}) := ((\mathbf{n}_1, \cdots, \mathbf{n}_N), (\boldsymbol{\omega}_1, \cdots, \boldsymbol{\omega}_N)) : \mathbb{R}_{\geq 0} \mapsto (\mathcal{S}^2)^N \times$

$(\mathbb{R}^3)^N$, and the control input $\mathbf{T} := (\mathbf{T}_1, \cdots, \mathbf{T}_N) : \mathbb{R}_{\geq 0} \mapsto (\mathbb{R}^3)^N$; where $\mathbf{x}(\cdot)$ evolves according to $\dot{\mathbf{x}}(t) = \mathbf{f}_{\mathbf{x}}(t, \mathbf{x}(t), \mathbf{T}(t))$ where

$$\mathbf{f}_{\mathbf{x}}(t, \mathbf{x}, \mathbf{T}) = (\mathbf{f}_{\mathbf{n}}(t, \mathbf{n}, \boldsymbol{\omega}), \mathbf{f}_{\boldsymbol{\omega}}(\boldsymbol{\omega}, \mathbf{T})) \in \mathbb{R}^{3N} \times \mathbb{R}^{3N}, \quad (3.4)$$

with $\mathbf{f}_{\mathbf{n}}(t, \mathbf{n}, \boldsymbol{\omega}) = (\mathbf{f}_{\mathbf{n}_1}(t, \mathbf{n}_1, \boldsymbol{\omega}_1), \cdots, \mathbf{f}_{\mathbf{n}_N}(t, \mathbf{n}_n, \boldsymbol{\omega}_N)) \in (\mathbb{R}^3)^N$ and $\mathbf{f}_{\boldsymbol{\omega}}(\boldsymbol{\omega}, \mathbf{T}) = (\mathbf{f}_{\boldsymbol{\omega}_1}(\boldsymbol{\omega}_1, \mathbf{T}_1), \cdots, \mathbf{f}_{\boldsymbol{\omega}_N}(\boldsymbol{\omega}_N, \mathbf{T}_N)) \in (\mathbb{R}^3)^N$.

4 Proposed Solution

4.1 Preliminaries

We first present some definitions and results from graph theory that are used in later sections [Godsil et al., 2001]. A graph $\mathcal{G} = \{\mathcal{N}, \mathcal{E}\}$ is said to be connected if there exists a path between any two vertices in $\mathcal{N}$. $\mathcal{G}$ is a tree if it is connected and it contains no cycles. An orientation on the graph $\mathcal{G}$ is the assignment of a direction to each edge $(i, j) \in \mathcal{E}$, where each edge vertex is either the tail or the head of the edge. For brevity, we denote $N = |\mathcal{N}|$, $M = |\mathcal{E}|$ and $\mathcal{M} = \{1, \cdots, M\}$. Consider the injective function $\bar{\kappa} : \{(i, j) \in \mathcal{E} : j > i\} \mapsto \mathcal{M}$ and the surjective function $\kappa : \mathcal{E} \mapsto \mathcal{M}$, which satisfy $\kappa(i, j) = \kappa(j, i) = \bar{\kappa}(i, j)$ for $j > i$; i.e., $\kappa(i, j)$ provides the edge number formed by neighboring agents i and j. The incidence matrix $B \in \mathbb{R}^{N \times M}$ of $\mathcal{G}$ is such that, for every $k \in \mathcal{M}$ and for $(i, j) = \bar{\kappa}^{-1}(k)$, $B_{ik} = 1$, $B_{jk} = -1$ and $B_{lk} = 0$ for all $l \in \mathcal{N} \backslash \{i, j\}$. Finally, for each edge $k \in \mathcal{M}$ and $(i, j) = \bar{\kappa}^{-1}(k)$, we denote ${}_k\mathbf{n} := \mathbf{n}_i$ and ${}_{\bar{k}}\mathbf{n} := \mathbf{n}_j$, i.e., we identify an agent by its node index but also by its edges' indexes (${}_k\mathbf{n}$ if $\mathbf{n}_i$ is the tail of edge k, and ${}_{\bar{k}}\mathbf{n}$ if $\mathbf{n}_i$ is the head of edge k). If $\mathcal{G}$ is connected but not a tree, then the null space of the incidence matrix, i.e., $\mathcal{N}(B)$, is non-empty, and it corresponds to the cycle space of $\mathcal{G}$ (Lemma 3.2 in [Guattery and Miller, 2000]). Let us now characterize $\mathcal{N}(B)$ for some specific network graphs with cycles.

Denote by $C \subseteq \{1, \cdots, M\}$ the set of indices corresponding to the edges that form a cycle. Consider a network graph with $n \in \mathbb{N}$ cycles, $\{C_i\}_{i=\{1,\cdots,n\}}$. We say that a cycle C_i is independent if $C_i \cap C_j = \emptyset$ for all $j \in \{1, \cdots, n\} \backslash \{i\}$. Additionally, we say that two cycles C_1 and C_2 share only one edge when $|C_1 \cap C_2| = 1$ and $C_1 \cup C_2$ contains edges from only the following three cycles (in $\{C_i\}_{i=\{1,\cdots,n\}}$): C_1, C_2 and $C_3 = C_1 \cup C_2 \backslash \{C_1 \cap C_2\}$, with $|C_3| = |C_1| + |C_2| - 2$. Figure 5(c) presents a graph with two cycles that share only one edge.

Proposition 4.1 Consider a graph $\mathcal{G}$ with n_1 independent cycles, $\{C_i\}_{i=\{1,\cdots,n_1\}}$, and n_2 pairs of cycles that share only one edge, $\{(C_i^1, C_i^2)\}_{i=\{1,\cdots,n_2\}}$. Then the null space of $B \otimes \mathrm{I}_n$ is given by $\mathcal{N}(B \otimes \mathrm{I}_n) = \{(\mathbf{e}_1, \cdots, \mathbf{e}_M) \in (\mathbb{R}^n)^M : \mathbf{e}_k = \pm\mathbf{e}_l, \forall k, l \in C_i, i = \{1, \cdots, n_1\}\} \cup \{(\mathbf{e}_1, \cdots, \mathbf{e}_M) \in (\mathbb{R}^n)^M : \mathbf{e}_k = \pm\mathbf{e}_l, \forall k, l \in C_i^1 \backslash \{C_i^1 \cap C_i^2\}, \mathbf{e}_p = \pm\mathbf{e}_q, \forall p, q \in C_i^2 \backslash \{C_i^1 \cap C_i^2\}, i = \{1, \cdots, n_2\}\}$.

Notice that for an incidence matrix $B \otimes \mathrm{I}_n$, with $B \in \mathbb{R}^{N \times M}$, there are M edges and each edge belongs to an n-dimensional space. With that in mind, and under the conditions of Proposition 4.1, it follows that the null space of $B \otimes \mathrm{I}_n$ is the space where all edges of an independent cycle have the same direction and norm (or are all zero); and all edges of pairs of cycles that share only one edge, except the one that is shared, have the same direction and norm (or are all zero). A proof of Proposition 4.1, including examples that illustrate its results, is found in [Pereira and Dimarogonas, 2016]. Proposition 4.1 is useful in a later section, where we prove that for network graphs that satisfy the conditions of the Proposition, the agents converge to a configuration where all unit vectors belong to a common plane.

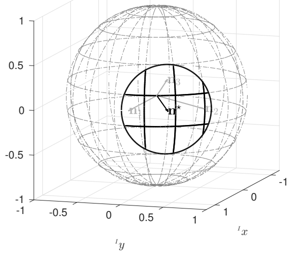

Fig. 2. Three unit vectors $\mathbf{n}_1$, $\mathbf{n}_2$ and $\mathbf{n}_3$ in a 30°-cone associated to the unit vector $\mathbf{n}^\star$.

We now present a definition and some results that will prove useful in a later section.

Definition 4.1 We say that a group of unit vectors $\mathbf{n} = (\mathbf{n}_1, \cdots, \mathbf{n}_N) \in (\mathcal{S}^2)^N$ belongs to an open (closed) $\alpha \in [0, \pi]$ cone, denoted by $\mathbf{n} \in \mathcal{C}(\alpha)$ ($\mathbf{n} \in \bar{\mathcal{C}}(\alpha)$), if there exists a unit vector $\mathbf{n}^\star \in \mathcal{S}^2$ such that $\mathbf{n}^{\star T}\mathbf{n}_i > \cos(\alpha)$ ($\mathbf{n}^{\star T}\mathbf{n}_i \geq \cos(\alpha)$) for all $i \in \mathcal{N}$.

The concept of α cone is exemplified in Fig. 2, with three unit vectors $\mathbf{n}_1$, $\mathbf{n}_2$ and $\mathbf{n}_3$ contained in a 30° cone formed by a unit vector $\mathbf{n}^\star$. In fact, any group of unit vectors contained in the sphere surface region marked in bold is contained in a 30° cone associated to the unit vector $\mathbf{n}^\star$.

Proposition 4.2 If $\mathbf{n} = (\mathbf{n}_1, \cdots, \mathbf{n}_N) \in \mathcal{C}(\alpha)$, for some $\alpha \in [0, \frac{\pi}{2}]$, then $\max_{(i,j)\in\mathcal{N}^2}(1 - \mathbf{n}_i^T\mathbf{n}_j) < 1 - \cos(2\alpha)$.

Proposition 4.3 If, given $\mathbf{n} = (\mathbf{n}_1, \cdots, \mathbf{n}_N) \in (\mathcal{S}^2)^N$, $\max_{(i,j)\in\mathcal{N}^2}(1 - \mathbf{n}_i^T\mathbf{n}_j) \leq 1 - \cos(\frac{2}{3}\alpha)$ holds for some $\alpha \in [0, \pi]$, then $\mathbf{n} \in \bar{\mathcal{C}}(\alpha)$.

Proofs of Propositions 4.2 and 4.3 are found in [Pereira and Dimarogonas, 2016].

4.2 Distance in $\mathcal{S}^2$

Definition 4.2 Consider a function $f \in \mathcal{C}^2((0, 2), \mathbb{R}_{>0})$, satisfying *i)* $f'(s) > 0 \forall s \in (0, 2)$, *ii)* $\lim_{s\to 0^+} f(s) = 0$, and *iii)* $\limsup_{s\to 0^+} f'(s), f''(s) < \infty$. Denote $f_2 := \lim_{s\to 2^-} f(s)$ and $f_0' := \lim_{s\to 0^+} f'(s)$. We say that: *1)* $f \in \mathcal{P}_0$ if $f_0' = 0$ and $f \in \mathcal{P}_{\bar{0}}$ if $f_0' \neq 0$; *2)* $f \in \mathcal{P}^\infty$ if $f_2 = \infty$, and $f \in \mathcal{P}^{\bar{\infty}}$ if $f_2 < \infty$; *3a)* $f \in \mathcal{P}^0$ if $f \in \mathcal{P}^{\bar{\infty}} \wedge \lim_{s\to 2^-} f'(s)\sqrt{2 - s} = 0$; *3b)* $f \in \mathcal{P}^{\bar{0}}$ if $f \in$

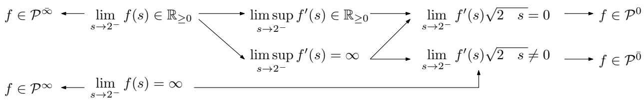

Fig. 3. Relation between properties of $f(\cdot)$ and the classes it belongs to.

$\mathcal{P}^{\bar{\infty}} \wedge \lim_{s\to 2^-} f'(s)\sqrt{2-s} \neq 0$; *4)* $f \in \bar{\mathcal{P}}$ if $f(\cdot)$ is of any of the previous classes.

Figure 4 illustrates the different classes introduced in Definition 4.2 while Fig. 3 illustrates how the properties that $f(\cdot)$ satisfies affects the classes it belongs to (see Remark G.1 in [Pereira and Dimarogonas, 2016]). In [Tron et al., 2012], the notion of *reshaping function* is introduced, whose definition is within the same spirit as that of Definition 4.2. For the rest of this manuscript, we assume that, for each edge $k \in \mathcal{M}$, there exists a function $d_k : \mathcal{S}^2 \times \mathcal{S}^2 \mapsto \mathbb{R}_{\geq 0}$ defined as $d_k(\mathbf{n}_1, \mathbf{n}_2) = f_k(1 - \mathbf{n}_1^T \mathbf{n}_2)$ and where $f_k \in \bar{\mathcal{P}}$; in particular, $f_k'(\cdot)$ plays the role of an edge weight. In e.g. [Moshtagh and Jadbabaie, 2007, Olfati-Saber, 2006], $f_k(s) = a_k s$ and $f_k'(s) = a_k$, for all $k \in \mathcal{M}$ (a_k is the weight of edge k and it is denoted by a_{ij} in [Olfati-Saber, 2006], where $(i, j) = \bar{\kappa}^{-1}(k)$). Denote also $\Omega^D_{\mathbf{n}} = \{\mathbf{n} \in (\mathcal{S}^2)^N : {}_k\mathbf{n}^T {}_{\bar{k}}\mathbf{n} \neq -1, \forall f_k \in \mathcal{P}^{\infty}\}$ and $D : \Omega^D_{\mathbf{n}} \mapsto \mathbb{R}_{\geq 0}$ defined as

$$D(\mathbf{n}) = \sum_{k=1}^{k=M} d_k({}_k\mathbf{n}, {}_{\bar{k}}\mathbf{n}) = \sum_{k=1}^{k=M} f_k(1 - {}_k\mathbf{n}^T {}_{\bar{k}}\mathbf{n}) \tag{4.1}$$

named, hereafter, total distance function of the network of unit vectors. Note that $D(\mathbf{n}) = 0 \Leftrightarrow \exists \mathbf{n}^\star \in \mathcal{S}^2 : \mathbf{n} = (\mathbf{1}_N \otimes \mathbf{n}^\star)$, which means Problem 3.1 is solved, if along a trajectory $\mathbf{x}(\cdot)$ of the closed loop system, $\lim_{t\to\infty} D(\mathbf{n}(t)) = 0$. Additionally, denote $\Omega^{\mathbf{e}_k}_{\mathbf{n}} = \{(\mathbf{n}_1, \mathbf{n}_2) \in (\mathcal{S}^2)^2 : \mathbf{n}_1^T \mathbf{n}_2 \neq -1 \text{ if } f_k \in \mathcal{P}^{\bar{0}}\}$ and $\mathbf{e}_k : \Omega^{\mathbf{e}_k}_{\mathbf{n}} \mapsto \mathbb{R}^3$ defined as

$$\mathbf{e}_k(\mathbf{n}_1, \mathbf{n}_2) = f_k'(1 - \mathbf{n}_1^T \mathbf{n}_2)\mathcal{S}(\mathbf{n}_1)\mathbf{n}_2, \tag{4.2}$$

to be the error of edge k, and for each $k \in \mathcal{M}$. And, finally, denote $\Omega^{\mathbf{e}}_{\mathbf{n}} = \{\mathbf{n} \in (\mathcal{S}^2)^N : {}_k\mathbf{n}^T {}_{\bar{k}}\mathbf{n} \neq -1, \forall f_k \in \mathcal{P}^{\bar{0}}\}$ and $\mathbf{e} : \mathbf{n} = (\mathbf{n}_1, \cdots, \mathbf{n}_N) \in \Omega^{\mathbf{e}}_{\mathbf{n}} \mapsto \mathbb{R}^{3M}$ defined as

$$\mathbf{e}(\mathbf{n}) = \begin{bmatrix} \mathbf{e}_1^T({}_1\mathbf{n}, {}_{\bar{1}}\mathbf{n}) & \cdots & \mathbf{e}_M^T({}_M\mathbf{n}, {}_{\bar{M}}\mathbf{n}) \end{bmatrix}^T. \tag{4.3}$$

If follows that

$$\frac{\partial D(\mathbf{n})}{\partial \mathbf{n}}^T \mathbf{f}_{\mathbf{n}}(t, \mathbf{n}, \boldsymbol{\omega}) = \boldsymbol{\omega}^T \mathcal{R}(t)^T (B \otimes \mathrm{I})\mathbf{e}(\mathbf{n}). \tag{4.4}$$

where $\mathcal{R}(\cdot) = \mathcal{R}_1(\cdot) \oplus \cdots \oplus \mathcal{R}_N(\cdot)$ (see Notation), which plays a role when studying the time derivative of (4.1) along a solution of the system with the vector field (3.4). Note that $\mathbf{e}_k(\mathbf{n}_1, \mathbf{n}_2)$ is well defined for all $(\mathbf{n}_1, \mathbf{n}_2) \in (\mathcal{S}^2)^2$ if $f_k \in \mathcal{P}^0$, and if $f_k \in \mathcal{P}^{\bar{0}}$, note that $\lim_{\mathbf{n}_2 \to \mathbf{n}_1} \mathbf{e}_k(\mathbf{n}_1, \mathbf{n}_2) = \lim_{s\to 2^-} f_k'(s)\sqrt{s(2-s)} \lim_{\mathbf{n}_2\to\mathbf{n}_1} \frac{\mathcal{S}(\mathbf{n}_1)\mathbf{n}_2}{\|\mathcal{S}(\mathbf{n}_1)\mathbf{n}_2\|}$ does not exist. Note that the total distance function (4.1) depends on $f_k(\cdot)$, for all $k \in \mathcal{M}$, while (4.3) depends on $f_k'(\cdot)$, for all $k \in \mathcal{M}$. As such, a distance function may or may not be defined when two unit vectors are diametrically opposed, depending on whether $f \in \mathcal{P}^{\infty}$ or $f \in \mathcal{P}^{\bar{\infty}}$; similarly, an edge error may or may not be defined when two unit vectors are diametrically opposed, depending on whether $f \in \mathcal{P}^0$ or $f \in \mathcal{P}^{\bar{0}}$. The domains of (4.1) and of (4.3) depend on the classes $f_k(\cdot)$ belongs to, for all $k \in \mathcal{M}$, and we emphasize that $\Omega^{\mathbf{e}}_{\mathbf{n}} \subseteq \Omega^D_{\mathbf{n}}$, since $f_k \in \mathcal{P}^{\infty} \Rightarrow f_k \in \mathcal{P}^{\bar{0}}$ (see Fig. 3). These domains play a role later on, since $D(\cdot)$ is used in constructing a Lyapunov function, while $\mathbf{e}(\cdot)$ is used in constructing the control law. As such, the Lyapunov function can be well defined, while the control law is not, while if the control law is well defined, so is the Lyapunov function. Consequently, it is important to guarantee that along trajectories of the closed-loop system, the control law is well defined. Additionally, notice that (4.2) provides some insight on why we denote $\mathbf{e}_k(\cdot,\cdot)$ as edge error of edge k. Indeed, if $f_k \in \bar{\mathcal{P}}, \forall k \in \mathcal{M}$, it follows that $\mathbf{e}_k({}_k\mathbf{n}, {}_{\bar{k}}\mathbf{n}) = \mathbf{0}$ implies that ${}_k\mathbf{n} = \pm_{\bar{k}}\mathbf{n}$, i.e., it implies that the neighbors that form edge k are either synchronized or diametrically opposed. Moreover, if $f_k \in \bar{\mathcal{P}} \,\forall k \in \mathcal{M}$, the distance between unit vectors is supremum when two unit vectors are diametrically opposed, i.e., for each $k \in \mathcal{M}$, (denote $\Omega = \{(\mathbf{n}_1, \mathbf{n}_2) \in \mathcal{S}^2 \times \mathcal{S}^2 : \mathbf{n}_1^T\mathbf{n}_2 = -1\}$) $\sup_{(\mathbf{n}_1,\mathbf{n}_2)\in\Omega} f_k(1 - \mathbf{n}_1^T\mathbf{n}_2) = \lim_{s\to 2^-} f_k(s) =: d_k^{\max}$. For convenience, denote

$$d^{\min} := \min_{k\in\mathcal{M}} d_k^{\max}, \tag{4.5}$$

which plays an important role in this and the following sections.

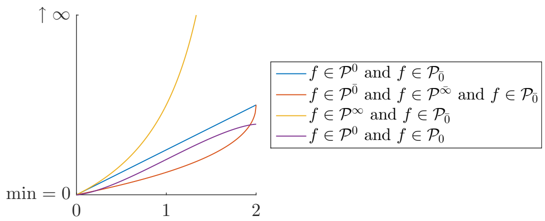

Fig. 4. Functions belonging to different classes as introduced in Definition 4.2: (from top to bottom in legend) $f(s) = s$, $f(s) = \pi^{-2}\arccos^2(1-s)$, $f(s) = \tan^2(0.5\arccos(1-s))$ and $f(s) = 0.25(\sqrt{s(2-s)}(s-1) + \arccos(1-s))$.

Proposition 4.4 Consider the total edge error in (4.3) and the total distance function in (4.1). Consider $\Omega'_{\mathbf{n}} : \mathbb{R}_{\geq 0} \mapsto 2^{\Omega^D_{\mathbf{n}}}$ defined as $\Omega'_{\mathbf{n}}(\bar{D}) = \{\mathbf{n} \in \Omega^D_{\mathbf{n}} : D(\mathbf{n}) \leq \bar{D}\}$, where $\Omega'_{\mathbf{n}}(\bar{D})$ is compact for all positive $\bar{D}$. Then, it follows that $\forall \bar{D} < d^{\min}$, $\max_{\mathbf{n}\in\Omega'_{\mathbf{n}}(\bar{D})} \|\mathbf{e}(\mathbf{n})\| < \infty$, and that there are no diametrically opposed neighbors, i.e., $|\{q \in \mathcal{M} : \forall \mathbf{n} \in \Omega'_{\mathbf{n}}(\bar{D}), {}_q\mathbf{n}^T {}_{\bar{q}}\mathbf{n} = -1\}| = 0$. If $f_k \in \mathcal{P}^0$ for all $k \in \mathcal{M}$, it follows that $\max_{\mathbf{n}\in\Omega^{\mathbf{e}}_{\mathbf{n}}} \|\mathbf{e}(\mathbf{n})\| = \max_{\mathbf{n}\in(\mathcal{S}^2)^N} \|\mathbf{e}(\mathbf{n})\| < \infty$; moreover, given $\bar{D} < p d^{\min}$ for some $p \in \mathcal{M}$, it follows that there are at most $p-1$ diametrically opposed neighbors, i.e., $|\{q \in \mathcal{M} : \forall \mathbf{n} \in \Omega'_{\mathbf{n}}(\bar{D}), {}_q\mathbf{n}^T {}_{\bar{q}}\mathbf{n} = -1\}| \leq p - 1$.

A proof is found in [Pereira and Dimarogonas, 2016].

4.3 Solution to Problem 3.1

In this section, we present the controllers for the torques of each agent. For each agent $i \in \mathcal{N}$, we design a controller that is a function of $|\mathcal{N}_i| + 1$ measurements: $|\mathcal{N}_i|$ measurements corresponding to the *distance* *measurements* between agent i and its $|\mathcal{N}_i|$ neighbors, and 1 measurement corresponding to the body frame angular velocity. More specifically, we assume that, at each time instant $t \geq 0$, each agent i measures $\mathcal{R}_i^T(t)\mathbf{n}_j(t) = \mathcal{R}_i^T(t)\mathcal{R}_j(t)\bar{\mathbf{n}}_j$ for each $j \in \mathcal{N}_i$; physically, this means that agent i knows $\bar{\mathbf{n}}_j$ (the *constant* unit vector that it is required to synchronize with), and that it can measure the projection of this unit vector on its orientation frame; each agent i must also measure $\boldsymbol{\omega}_i(t)$, which does not require an inertial reference frame. For convenience denote $\mathcal{N}_i = \{i_1, \cdots, i_{|\mathcal{N}_i|}\}$, and, given $\bar{\mathbf{n}}_i \in \mathcal{S}^2$, denote $\Omega_{\mathbf{n}_i} = \{(\mathbf{n}_{i_1}, \cdots, \mathbf{n}_{i_{|\mathcal{N}_i|}}) \in (\mathcal{S}^2)^{|\mathcal{N}_i|} : \bar{\mathbf{n}}_i^T\mathbf{n}_{i_l} \neq -1, \forall l \in \{1, \cdots, |\mathcal{N}_i|\} \wedge f_{\kappa(i,i_l)} \in \mathcal{P}^{\bar{0}}\}$ which provides the domain where the control law for agent i is well defined (recall that if $f_k \in \mathcal{P}^{\bar{0}}$, for some $k \in \mathcal{M}$, then (4.2) is not defined when two unit vectors are diametrically opposed). We then propose, for each agent $i \in \mathcal{N}$, the decentralized control law $\mathbf{T}_i^{cl} : (\boldsymbol{\nu}_i, \boldsymbol{\omega}_i) = ((\mathcal{R}_i^T\mathbf{n}_{i_1}, \cdots, \mathcal{R}_i^T\mathbf{n}_{i_{|\mathcal{N}_i|}}), \boldsymbol{\omega}_i) \in \Omega_{\mathbf{n}_i} \times \mathbb{R}^3 \mapsto \mathbb{R}^3$ defined as

$$\mathbf{T}_i^{cl}(\boldsymbol{\nu}_i, \boldsymbol{\omega}_i) = -\boldsymbol{\sigma}(\boldsymbol{\omega}_i) - \textstyle\sum_{l=1}^{l=|\mathcal{N}_i|} \mathbf{e}_{\kappa(i,i_l)}\left(\bar{\mathbf{n}}_i, \mathcal{R}_i^T\mathbf{n}_{i_l}\right), \quad (4.6)$$

with $\boldsymbol{\sigma} : \mathbb{R}^3 \mapsto \mathbb{R}^3$ such that $\exists \sigma \in \mathcal{C}^1(\mathbb{R}_{>0}, \mathbb{R}_{>0}) : \boldsymbol{\sigma}(\mathbf{x}) = \sigma(\|\mathbf{x}\|)\frac{\mathbf{x}}{\|\mathbf{x}\|}$ with $\sigma(0) = 0$. The timed control laws for each agent $i \in \mathcal{N}$ are then $\mathbf{T}_i : \mathbb{R}_{\geq 0} \mapsto \mathbb{R}^3$ given by

$$\mathbf{T}_i(t) = \mathbf{T}_i^{cl}((\mathcal{R}_i^T(t)\mathbf{n}_{j_1}(t), \cdots, \mathcal{R}_i^T(t)\mathbf{n}_{j_{|\mathcal{N}_i|}}(t)), \boldsymbol{\omega}_i(t)). \quad (4.7)$$

The proposed torque control law exhibits the following properties. The controller function in (4.7) is decentralized in the sense that it does not depend on the measurement of the global state. Also, (4.7) can be implemented without the knowledge of an inertial orientation frame, since measuring $\mathcal{R}_i^T(t)\mathcal{R}_{i_l}(t)\bar{\mathbf{n}}_{i_l}$, at every time instant $t \geq 0$ and for all $l \in \{1, \cdots, |\mathcal{N}_i|\}$, requires only the measurement of the projection of $\bar{\mathbf{n}}_{i_l}$ in agent's i body orientation frame; while $\boldsymbol{\omega}_i(t)$ is also measured in agent's i body orientation frame. Finally, notice that $\|\mathbf{T}_i(\cdot)\| \leq \sigma^{\max} + |\mathcal{N}_i| \max_{j\in\mathcal{N}_i} \sup_{0<s<2} f'_{\kappa(i,j)}(s)$ ($\sigma^{\max} = \sup_{\mathbf{x}\in\mathbb{R}^3} \|\boldsymbol{\sigma}(\mathbf{x})\| \leq \infty$). As such, the proposed control law, for each agent i, can be implemented with bounded actuation provided that $\sigma^{\max} < \infty$ and that $f_{\kappa(i,j)} \in \mathcal{P}^0$ for all $j \in \mathcal{N}_i$. Notice that $\sum_{k\in\mathcal{M}'\subseteq\mathcal{M}} \|\mathbf{e}_k(\cdot,\cdot)\| \leq \sum_{k\in\mathcal{M}} \|\mathbf{e}_k(\cdot,\cdot)\| \leq \sqrt{M}\|\mathbf{e}(\cdot)\|$, and, therefore, for any $\mathcal{R}_i \in \mathcal{SO}(3)$, and for all $\mathbf{x} \in \Omega_{\mathbf{n}}^{\mathbf{e}} \times \mathbb{R}^{3N}$,

$$\|\mathbf{T}_i^{cl}((\mathcal{R}_i^T\mathbf{n}_{i_1}, \cdots, \mathcal{R}_i^T\mathbf{n}_{i_{|\mathcal{N}_i|}}), \boldsymbol{\omega}_i)\| \leq \sigma'^{\max}\|\boldsymbol{\omega}_i\| + \sqrt{M}\|\mathbf{e}(\mathbf{n})\| \quad (4.8)$$

which is made use of later in this section. By combining (4.6) for all $i \in \mathcal{N}$, we obtain the complete control law $\mathbf{T}^{cl} : (t, \mathbf{x}) = (t, (\mathbf{n}, \boldsymbol{\omega})) \in \mathbb{R}_{\geq 0} \times (\Omega_{\mathbf{n}}^{\mathbf{e}} \times \mathbb{R}^{3N}) \mapsto \mathbb{R}^{3N}$, which is given by

$$\mathbf{T}^{cl}(t, \mathbf{x}) = -\Sigma(\boldsymbol{\omega}) - \mathcal{R}^T(t)(B \otimes \mathrm{I})\mathbf{e}(\mathbf{n}), \quad (4.9)$$

where $\mathcal{R}(\cdot) = \mathcal{R}_1(\cdot) \oplus \cdots \oplus \mathcal{R}_N(\cdot)$ (see Notation), and $\Sigma(\boldsymbol{\omega}) = [\boldsymbol{\sigma}^T(\boldsymbol{\omega}_1) \cdots \boldsymbol{\sigma}^T(\boldsymbol{\omega}_N)]^T$. For the remainder of this paper, we dedicate efforts in studying the equilibria configurations induced by this control law (for different types of graphs), their stability, and what is the effect of the chosen distance functions. Notice that (4.9) is defined on $\mathbb{R}_{\geq 0} \times \Omega_{\mathbf{n}}^{\mathbf{e}} \times \mathbb{R}^{3N}$. As such, when $f_k \in \mathcal{P}^0\ \forall k \in \mathcal{M}$, $\Omega_{\mathbf{n}}^{\mathbf{e}} = (\mathcal{S}^2)^N$, and the analysis is simpler; when, however, $\exists k \in \mathcal{M} : f_k \in \mathcal{P}^{\bar{0}}$, then $\Omega_{\mathbf{n}}^{\mathbf{e}} \subset (\mathcal{S}^2)^N$ (where $\Omega_{\mathbf{n}}^{\mathbf{e}}$ is open), and it is necessary to guarantee that a trajectory $\mathbf{x}(\cdot)$ of $\dot{\mathbf{x}}(t) = \mathbf{f}_{\mathbf{x}}(t, \mathbf{x}(t), \mathbf{T}^{cl}(t, \mathbf{x}(t)))$ never approaches the boundary of $\Omega_{\mathbf{n}}^{\mathbf{e}} \times \mathbb{R}^{3N}$.

4.4 Constrained Torque

A natural constraint in a physical system is to require the torque provided by agent i to be orthogonal to $\bar{\mathbf{n}}_i$. In satellites, thrusters that provide torque along $\bar{\mathbf{n}}_i$ might be unavailable; also, controlling the space orthogonal to $\bar{\mathbf{n}}_i$ can be left as an additional degree of freedom, in order to accomplish some other control objectives. However, the control laws proposed in (4.6) require full torque actuation, in particular, (4.6) requires each agent to provide torque on the plane orthogonal to $\bar{\mathbf{n}}_i$. Indeed, since $\mathbf{n}_1^T\mathbf{e}_k(\mathbf{n}_1, \cdot) = 0$, $\forall \mathbf{n}_1 \in \mathcal{S}^2, \forall k \in \mathcal{M}$ (see (4.2)), it follows that, for all $i \in \mathcal{N}$, $\bar{\mathbf{n}}_i^T\mathbf{T}_i^{cl}(\cdot, \boldsymbol{\omega}_i) = \bar{\mathbf{n}}_i^T\boldsymbol{\sigma}(\boldsymbol{\omega}_i)$ for all $\boldsymbol{\omega}_i \in \mathbb{R}^3$, which is not necessarily 0. In short, previously, we provided control laws $\mathbf{T}_i^{cl} : \Omega_{\mathbf{n}_i} \times \mathbb{R}^3 \mapsto \mathbb{R}^3$ which require full torque by each agent $i \in \mathcal{N}$, and in this section we provide constrained control laws $\bar{\mathbf{T}}_i^{cl} : \Omega_{\mathbf{n}_i} \times \mathbb{R}^3 \mapsto \{\mathbf{z} \in \mathbb{R}^3 : \mathbf{z}^T\bar{\mathbf{n}}_i = 0\}$, i.e., control laws which do not require torque along $\bar{\mathbf{n}}_i$. Let us anticipate a future result by announcing that the constrained control law can only be used by agent $i \in \mathcal{N}$ when the unit vector to be synchronized by agent $i \in \mathcal{N}$, namely $\bar{\mathbf{n}}_i$, is a principal axis of that agent (i.e., when $\bar{\mathbf{n}}_i$ is an eigenvector of J_i). Consider then $\bar{\mathbf{T}}_i^{cl} : (\boldsymbol{\nu}_i, \boldsymbol{\omega}_i) = ((\mathcal{R}_i^T\mathbf{n}_{i_1}, \cdots, \mathcal{R}_i^T\mathbf{n}_{i_{|\mathcal{N}_i|}}), \boldsymbol{\omega}_i) \in \Omega_{\mathbf{n}_i} \times \mathbb{R}^3 \mapsto \{\mathbf{z} \in \mathbb{R}^3 : \mathbf{z}^T\bar{\mathbf{n}}_i = 0\}$ defined as (see Notation for definition of $\Pi(\cdot)$)

$$\begin{aligned}\bar{\mathbf{T}}_i^{cl}(\boldsymbol{\nu}_i, \boldsymbol{\omega}_i) &= \Pi(\bar{\mathbf{n}}_i)\,\mathbf{T}_i^{cl}(\boldsymbol{\nu}_i, \boldsymbol{\omega}_i) \\ &\overset{(4.6)}{=} -\boldsymbol{\sigma}(\Pi(\bar{\mathbf{n}}_i)\,\boldsymbol{\omega}_i) - \sum_{l=1}^{l=|\mathcal{N}_i|} \mathbf{e}_{\kappa(i,i_l)}\left(\bar{\mathbf{n}}_i, \mathcal{R}_i^T\mathbf{n}_{i_l}\right) \quad (4.10)\end{aligned}$$

Additionally, consider a partition of $\mathcal{N}$, i.e., $\bar{\mathcal{L}} \cup \mathcal{L} = \mathcal{N}$ with $\bar{\mathcal{L}} \cap \mathcal{L} = \emptyset$; where $\bar{\mathcal{L}}$ is a subset (possibly empty) of the agents whose unit vector to synchronize is an eigenvector of their moment of inertia, i.e., $\bar{\mathcal{L}} \subseteq \{i \in \mathcal{N} : \exists \lambda_i \text{ s.t. } J_i\bar{\mathbf{n}}_i = \lambda_i\bar{\mathbf{n}}_i\}$. Then we propose the complete control law $\bar{\mathbf{T}}^{cl} : (t, \mathbf{x}) \in \mathbb{R}_{\geq 0} \times (\Omega_{\mathbf{n}}^{\mathbf{e}} \times \mathbb{R}^{3N}) \mapsto \mathbb{R}^{3N}$ defined as

$$\begin{cases}(\mathbf{e}_i \otimes \mathbf{1}_3)^T\bar{\mathbf{T}}^{cl}(t, \mathbf{x}) = \bar{\mathbf{T}}_i^{cl}((\mathcal{R}_i^T(t)\mathbf{n}_{i_1}, \cdots, \mathcal{R}_i^T(t)\mathbf{n}_{i_{|\mathcal{N}_i|}}), \boldsymbol{\omega}_i)\ \forall i \in \bar{\mathcal{L}} \\ (\mathbf{e}_i \otimes \mathbf{1}_3)^T\bar{\mathbf{T}}^{cl}(t, \mathbf{x}) = \mathbf{T}_i^{cl}((\mathcal{R}_i^T(t)\mathbf{n}_{i_1}, \cdots, \mathcal{R}_i^T(t)\mathbf{n}_{i_{|\mathcal{N}_i|}}), \boldsymbol{\omega}_i)\ \forall i \in \mathcal{L},\end{cases} \quad (4.11)$$

i.e., for agents whose unit vector to synchronize is a principal axis, either control law (4.6) or (4.10) is chosen, and, for all other agents, control law (4.6) is chosen. As such, agents whose unit vector to synchronize is a principal axis have an option between using full torque control or constrained torque control. The disadvantage with the control law in (4.10) is that, along a trajectory of the closed-loop system, and for all $i \in \bar{\mathcal{L}}$, $\lim_{t\to\infty} \bar{\mathbf{n}}_i^T\boldsymbol{\omega}_i(t)$ is not guaranteed to exist and be 0; i.e., an agent that opts for (4.10) can asymptotically spin, with non-zero angular velocity, around $\bar{\mathbf{n}}_i$ (nonetheless, we can guarantee that $\sup_{t\geq 0} \|\boldsymbol{\omega}_i(t)\| < \infty \Rightarrow \sup_{t\geq 0} |\bar{\mathbf{n}}_i^T\boldsymbol{\omega}_i(t)| < \infty$, i.e., if an agent applies (4.10) it never spins infinitely fast around its principal axis $\bar{\mathbf{n}}_i$).

4.5 Lyapunov Function

In addition to the total distance function of the network (4.1), let us also define the total rotational kinetic energy of the network $H : \boldsymbol{\omega} = (\boldsymbol{\omega}_1, \cdots, \boldsymbol{\omega}_N) \in (\mathbb{R}^3)^N \mapsto \mathbb{R}_{\geq 0}$ as

$$H(\boldsymbol{\omega}) = \frac{1}{2} \sum\nolimits_{i=1}^{i=N} \boldsymbol{\omega}_i^T J_i \boldsymbol{\omega}_i, \tag{4.12}$$

which satisfies $\frac{\partial H(\boldsymbol{\omega})}{\partial \boldsymbol{\omega}}^T \mathbf{f}_{\boldsymbol{\omega}}(\boldsymbol{\omega}, \mathbf{T}) = \sum_{i=1}^{i=N} \boldsymbol{\omega}_i^T J_i \mathbf{f}_{\boldsymbol{\omega}_i}(\boldsymbol{\omega}_i, \mathbf{T}_i) = \boldsymbol{\omega}^T \mathbf{T}$, for all $(\boldsymbol{\omega}, \mathbf{T}) \in (\mathbb{R}^{3N})^2$. Combining (4.1) and (4.12), consider then the Lyapunov function $V : \mathbf{x} = (\mathbf{n}, \boldsymbol{\omega}) \in \Omega_{\mathbf{n}}^D \times \mathbb{R}^{3N} \mapsto \mathbb{R}_{\geq 0}$ defined as

$$V(\mathbf{x}) = D(\mathbf{n}) + H(\boldsymbol{\omega}), \tag{4.13}$$

and the function $W : \boldsymbol{\omega} = (\boldsymbol{\omega}_1, \cdots, \boldsymbol{\omega}_N) \in (\mathbb{R}^3)^N \mapsto \mathbb{R}_{\geq 0}$ defined as

$$W(\boldsymbol{\omega}) = \sum_{i \in \mathcal{L}} \boldsymbol{\omega}_i^T \boldsymbol{\sigma}(\boldsymbol{\omega}_i) + \sum_{j \in \bar{\mathcal{L}}} \boldsymbol{\omega}_j^T \Pi(\bar{\mathbf{n}}_j) \boldsymbol{\sigma}(\boldsymbol{\omega}_j). \tag{4.14}$$

It follows that, along a trajectory $\mathbf{x}(\cdot)$ of $\dot{\mathbf{x}}(t) = \mathbf{f}_{\mathbf{x}}(t, \mathbf{x}(t), \mathbf{T}^{cl}(t, \mathbf{x})), \dot{V}(\mathbf{x}(t)) = \dot{D}(\mathbf{n}(t)) + \dot{H}(\boldsymbol{\omega}(t)) \overset{(4.4),(4.9)}{=} -W(\boldsymbol{\omega}(t)) \leq 0, \forall t \geq 0$. Moreover, along that same trajectory $\mathbf{x}(\cdot)$, it follows that

$$|\dot{W}(\boldsymbol{\omega}(t))| \leq \sum_{1=1}^{i=N} (\sigma_s + \sigma'^{\max})^T \|\boldsymbol{\omega}_i(t)\| f_{\boldsymbol{\omega}_i}^{\infty}(\mathbf{x}(t)), \tag{4.15}$$

($\sigma_s = \sup_{\mathbf{x} \in \mathbb{R}^3 \setminus \{\mathbf{0}\}} \frac{\|\boldsymbol{\sigma}(\mathbf{x})\|}{\|\mathbf{x}\|} < \infty$ and $\sigma'^{\max} = \sup_{\mathbf{x} \in \mathbb{R}^3} \|\frac{\partial \boldsymbol{\sigma}(\mathbf{x})}{\partial \mathbf{x}}\| < \infty$), where, for every $i \in \mathcal{N}$,

$$\|\mathbf{f}_{\boldsymbol{\omega}_i}(\boldsymbol{\omega}_i, \mathbf{T}_i^{cl}(\cdot))\| \overset{(3.3)}{\leq} \frac{1}{\lambda_{\min}(J_i)} \left(\mathbf{T}_i^{cl}(\cdot) + \lambda_{\max}(J_i) \|\boldsymbol{\omega}_i\|^2 \right)$$
$$\overset{(4.8)}{\leq} \frac{1}{\lambda_{\min}(J_i)} \left(\sigma'^{\max} \|\boldsymbol{\omega}_i\| + \sqrt{M} \|\mathbf{e}(\mathbf{n})\| + \lambda_{\max}(J_i) \|\boldsymbol{\omega}_i\|^2 \right) =: f_{\boldsymbol{\omega}_i}^{\infty}(\mathbf{x}) \tag{4.16}$$

It also follows that, along that same trajectory, and for every $i \in \mathcal{N}$ (we omit the time dependencies below)

$$\ddot{\boldsymbol{\omega}}_i = -J_i^{-1} \left(\mathcal{S}(\dot{\boldsymbol{\omega}}_i) J_i \boldsymbol{\omega}_i + \mathcal{S}(\boldsymbol{\omega}_i) J_i \dot{\boldsymbol{\omega}}_i + D\boldsymbol{\sigma}(\boldsymbol{\omega}_i) \dot{\boldsymbol{\omega}}_i \right) +$$
$$J_i^{-1} \mathcal{R}_i^T \mathcal{S}(\mathbf{n}_i) \sum_{j \in \mathcal{N}_i} (f'(\cdot) \mathrm{I} - f''(\cdot) \mathbf{n}_j \mathbf{n}_i^T) \mathcal{S}(\mathbf{n}_j) (\mathcal{R}_i \boldsymbol{\omega}_i - \mathcal{R}_j \boldsymbol{\omega}_j). \tag{4.17}$$

It follows from (4.15), (4.16) and (4.17) that if $\sup_{t \geq 0} \|\mathbf{e}(\mathbf{n}(t))\| < \infty$ and $\sup_{t \geq 0} \|\boldsymbol{\omega}_i(t)\| < \infty$, then $\sup_{t \geq 0} |\dot{W}(\boldsymbol{\omega}(t))| < \infty$ and $\sup_{t \geq 0} \|\ddot{\boldsymbol{\omega}}_i(t)\| < \infty$; this in turn implies that $W(\boldsymbol{\omega}(\cdot))$ and $\dot{\boldsymbol{\omega}}_i(\cdot)$ are uniformly continuous, which plays a role in proving that $\lim_{t \to \infty} W(\boldsymbol{\omega}(t)) = 0$ and that $\lim_{t \to \infty} \dot{\boldsymbol{\omega}}_i(t) = 0$.

Proposition 4.5 Consider the vector field (3.4), the control law (4.11), and a trajectory $\mathbf{x}(\cdot)$ of $\dot{\mathbf{x}}(t) = \mathbf{f}_{\mathbf{x}}(t, \mathbf{x}(t), \bar{\mathbf{T}}^{cl}(t, \mathbf{x}(t)))$. If $\mathbf{x}(0) \in \Omega_{\mathbf{x}}^0 = \{\mathbf{x} \in \Omega_{\mathbf{n}}^D \times \mathbb{R}^{3N} : V(\mathbf{x}) < d^{\min}\}$, then $\lim_{t \to \infty} (B \otimes \mathrm{I}) \mathbf{e}(\mathbf{n}(t)) = \mathbf{0}$, $\lim_{t \to \infty} \boldsymbol{\omega}_i(t) = \mathbf{0}$ for $i \in \mathcal{L}$ and $\lim_{t \to \infty} \Pi(\bar{\mathbf{n}}_j) \boldsymbol{\omega}_j(t) = \mathbf{0}$ for $j \in \bar{\mathcal{L}}$. Moreover, $\sup_{t \geq 0} |\bar{\mathbf{n}}_j^T \boldsymbol{\omega}_j(t)| < \infty$ for $j \in \bar{\mathcal{L}}$.

Proof For brevity, we say $\mathbf{f} : \mathbb{R}_{\geq 0} \mapsto \mathbb{R}^n$ is bounded, if $\sup_{t \geq 0} \|\mathbf{f}(t)\| < \infty$; we say $\mathbf{f} : \mathbb{R}_{\geq 0} \mapsto \mathbb{R}^n$ converges to a constant, if $\exists \mathbf{f}^{\infty} \in \mathbb{R}^n : \lim_{t \to \infty} \mathbf{f}(t) = \mathbf{f}^{\infty}$. Let us provide a brief summary for the proof. First, we prove that, along a trajectory $\mathbf{x}(\cdot)$, $\|\boldsymbol{\omega}(\cdot)\|$ and $\|\mathbf{e}(\mathbf{n}(\cdot))\|$ are bounded. This, in turn, guarantees uniform continuity of $\dot{V}(\mathbf{x}(\cdot))$ and of $\dot{\boldsymbol{\omega}}(\cdot)$. And finally, since both $V(\mathbf{x}(\cdot))$ and $\boldsymbol{\omega}(\cdot)$ converge to a constant, we invoke Barbalat's lemma (see [Slotine and Li, 1991], Lemma 4.2) to conclude that $\mathbf{e}(\mathbf{n}(\cdot))$ converges to the null space of $B \otimes \mathrm{I}$.

Recall then the functions in (4.13) and (4.14). Since $\dot{V}(\mathbf{x}(\cdot)) \leq -W(\boldsymbol{\omega}(\cdot)) \leq 0$, it follows that $V(\mathbf{x}(\cdot)) \leq V(\mathbf{x}(0)) < d^{\min}$. Therefore $D(\mathbf{n}(\cdot)) < d^{\min}$ and $H(\boldsymbol{\omega}(\cdot)) < d^{\min}$. From $D(\mathbf{n}(\cdot)) < d^{\min}$, it follows, with the help of Proposition 4.4, that $\mathbf{e}(\mathbf{n}(\cdot))$ is bounded; while from $H(\boldsymbol{\omega}(\cdot)) < d^{\min}$, it follows that $\boldsymbol{\omega}(\cdot)$ is also bounded. From boundedness of $\mathbf{e}(\mathbf{n}(\cdot))$ and $\boldsymbol{\omega}(\cdot)$, it follows that $\bar{\mathbf{T}}^{cl}(\cdot, \mathbf{x}(\cdot))$ is bounded (see (4.11) and (4.9)); that $\|\dot{\boldsymbol{\omega}}_i(\cdot)\| \leq f_{\boldsymbol{\omega}_i}^{\infty}(\mathbf{x}(\cdot))$ is bounded (see (4.16)); that $|\ddot{V}(\mathbf{x}(\cdot))| = |\dot{W}(\boldsymbol{\omega}(\cdot))|$ is bounded (see (4.15)); and, finally, that $\ddot{\boldsymbol{\omega}}_i(\cdot)$ is bounded (see (4.17)). The previous conclusions imply that $\dot{V}(\mathbf{x}(\cdot))$ and that $\dot{\boldsymbol{\omega}}(\cdot)$ are both uniformly continuous. Since $V(\cdot) \geq 0$ and $\dot{V}(\mathbf{x}(\cdot)) \leq -W(\boldsymbol{\omega}(\cdot)) \leq 0$, it follows that $V(\mathbf{x}(\cdot))$ converges to a constant; by Barbalat's lemma, uniform continuity of $\dot{V}(\mathbf{x}(\cdot))$ then implies that $\dot{V}(\mathbf{x}(\cdot)) = -W(\boldsymbol{\omega}(\cdot))$ converges to 0. As such, it follows from (4.14), that $\boldsymbol{\omega}_i(\cdot)$ converges to $\mathbf{0}$, for all $i \in \mathcal{L}$, while $\Pi(\bar{\mathbf{n}}_j) \boldsymbol{\omega}_j(\cdot)$ converges to $\mathbf{0}$, for all $j \in \bar{\mathcal{L}}$; also, notice that

$$\lim_{t \to \infty} \Pi(\bar{\mathbf{n}}_j) \boldsymbol{\omega}_j(t) = \mathbf{0} \Rightarrow \lim_{t \to \infty} (\boldsymbol{\omega}_j(t) - \bar{\mathbf{n}}_j (\bar{\mathbf{n}}_j^T \boldsymbol{\omega}_j(t))) = \mathbf{0}. \tag{4.18}$$

Let us now study agents in $\mathcal{L}$ and $\bar{\mathcal{L}}$ separately. Also, for convenience, and with some abuse of notation, denote $\mathbf{T}_i^{cl}(t) = (\mathbf{e}_i \otimes \mathbf{1}_3)^T \bar{\mathbf{T}}^{cl}(t, \mathbf{x}(t))$, for $i \in \mathcal{L}$, and $\bar{\mathbf{T}}_j^{cl}(t) = (\mathbf{e}_j \otimes \mathbf{1}_3)^T \bar{\mathbf{T}}^{cl}(t, \mathbf{x}(t))$, for $j \in \bar{\mathcal{L}}$. For $i \in \mathcal{L}$ (for which (4.6) is the chosen control law), and again by Barbalat's lemma, convergence of $\boldsymbol{\omega}_i(\cdot)$ to $\mathbf{0}$ and uniform continuity of $\dot{\boldsymbol{\omega}}_i(\cdot)$ imply that $\dot{\boldsymbol{\omega}}_i(\cdot) = \mathbf{f}_{\boldsymbol{\omega}_i}(\boldsymbol{\omega}_i(\cdot), \mathbf{T}_i^{cl}(\cdot))$ converges to $\mathbf{0}$; since $\boldsymbol{\omega}_i(\cdot)$ converges to $\mathbf{0}$, so does $\mathbf{T}_i^{cl}(\cdot, \mathbf{x}(\cdot))$ (see 3.3). Now, for $j \in \bar{\mathcal{L}}$ (for which (4.10) is the chosen control law), and once again by Barbalat's lemma, convergence of $\Pi(\bar{\mathbf{n}}_j) \boldsymbol{\omega}_j(\cdot)$ to $\mathbf{0}$ and uniform continuity of $\frac{d}{dt}(\Pi(\bar{\mathbf{n}}_j) \boldsymbol{\omega}(t)) = \Pi(\bar{\mathbf{n}}_j) \dot{\boldsymbol{\omega}}(t)$ implies that $\Pi(\bar{\mathbf{n}}_j) \dot{\boldsymbol{\omega}}(\cdot)$ converges to $\mathbf{0}$, and therefore

$$\lim_{t \to \infty} \Pi(\bar{\mathbf{n}}_j) \dot{\boldsymbol{\omega}}_j(t) = \mathbf{0} \Rightarrow \lim_{t \to \infty} (\dot{\boldsymbol{\omega}}_j(t) - \bar{\mathbf{n}}_j (\bar{\mathbf{n}}_j^T \dot{\boldsymbol{\omega}}_j(t))) = \mathbf{0}, \tag{4.19}$$

Now, recall (3.2) where $J_j \dot{\boldsymbol{\omega}}_j(t) = -\mathcal{S}(\boldsymbol{\omega}_j(t)) J_j \boldsymbol{\omega}_j(t) + \bar{\mathbf{T}}_j^{cl}(t)$, and, from (4.18) and (4.19), it follows that

$$\lim_{t \to \infty} \left(J_j \bar{\mathbf{n}}_j (\bar{\mathbf{n}}_j^T \dot{\boldsymbol{\omega}}_j(t)) + \mathcal{S}(\bar{\mathbf{n}}_j) J_j \bar{\mathbf{n}}_j (\bar{\mathbf{n}}_i^T \boldsymbol{\omega}_j(t))^2 - \bar{\mathbf{T}}_j^{cl}(t) \right) = \mathbf{0}$$
$$\overset{J_j \bar{\mathbf{n}}_j = \lambda_j \bar{\mathbf{n}}_j}{\Rightarrow} \lim_{t \to \infty} \left(\lambda_j \bar{\mathbf{n}}_j (\bar{\mathbf{n}}_j^T \dot{\boldsymbol{\omega}}_j(t)) - \bar{\mathbf{T}}_j^{cl}(t) \right) = \mathbf{0} \tag{4.20}$$

If we take the inner product of (4.20) with $\bar{\mathbf{n}}_j$, and since $\bar{\mathbf{T}}_j^{cl}(\cdot) \perp \bar{\mathbf{n}}_j$, it follows that $\lim_{t \to \infty} (\bar{\mathbf{n}}_j^T \dot{\boldsymbol{\omega}}_i(t)) = 0$. As such, it follows from (4.20) that $\bar{\mathbf{T}}_j^{cl}(\cdot)$ converges to $\mathbf{0}$ for all $j \in \bar{\mathcal{L}}$. Now to summarize, recall that, for all $i \in \mathcal{L}$, both $\boldsymbol{\omega}_i(\cdot)$ and $\mathbf{T}_i^{cl}(\cdot, \mathbf{x}(\cdot))$ converge to $\mathbf{0}$, which implies, from (4.6), that $\sum_{l=1}^{l=|\mathcal{N}_i|} \mathbf{e}_{\kappa(i,i_l)} \left(\bar{\mathbf{n}}_i, \mathcal{R}_i(\cdot)^T \mathbf{n}_{i_l}(\cdot) \right)$ converges to $\mathbf{0}$. On the other hand, for all $j \in \bar{\mathcal{L}}$, both $\Pi(\bar{\mathbf{n}}_j) \boldsymbol{\omega}_j(\cdot)$ and $\bar{\mathbf{T}}_j^{cl}(\cdot, \mathbf{x}(\cdot))$ converge to zero, which implies, from (4.10), that $\sum_{l=1}^{l=|\mathcal{N}_j|} \mathbf{e}_{\kappa(j,j_l)}\left(\bar{\mathbf{n}}_j, \mathcal{R}_j(\cdot)^T \mathbf{n}_{j_l}(\cdot)\right)$ converges to $\mathbf{0}$. All together, it implies that $(B\otimes \mathrm{I})\mathbf{e}(\mathbf{n}(\cdot))$ converges to $\mathbf{0}$. Finally, $\sup_{t\geq 0} |\bar{\mathbf{n}}_j^T \boldsymbol{\omega}_j(t)| < \infty$ since $\boldsymbol{\omega}(\cdot)$ is bounded ($H(\boldsymbol{\omega}(\cdot)) < d^{\min}$). $\square$

Notice that $d^{\min}$, in (4.5), is a design parameter, and, therefore, the domain of attraction in Proposition 4.5 can be made larger by increasing this parameter. More specifically, $d^{\min}$ increases the domain of attraction in the state space related to $\boldsymbol{\omega}$, which is clearer in the next corollary.

Corollary 4.1 Proposition 4.5 holds if $r := \frac{H(\boldsymbol{\omega}(0))}{d^{\min}} < 1$ and if

$$\mathbf{n}(0) \in \mathcal{C}\left(\tfrac{1}{2}\arccos\left(1 - \min_{k\in\mathcal{M}} f_k^{-1}\left(d^{\min}\tfrac{1-r}{M}\right)\right)\right), \quad (4.21)$$

where $d^{\min} = \min_{k\in\mathcal{M}} \lim_{s\to 2^-} f_k(s)$. If $f_k \in \mathcal{P}^\infty$ for all $k \in \mathcal{M}$, then $d^{\min} = \infty$ and (4.21) reduces to $\mathbf{n}(0) \in \mathcal{C}(\frac{\pi}{2})$.

For proving the latter Corollary, it suffices to check that the conditions of Proposition 4.5 hold [Pereira and Dimarogonas, 2016]. Corollary 4.1 states that if the total kinetic energy is *small*, and if all neighbors are initially contained in a *small* cone, then synchronization is guaranteed. Moreover, if $d^{\min} = \infty$ and if all neighbors are initially contained in an open $\frac{\pi}{2}$-cone, then synchronization is also guaranteed.

Proposition 4.6 Consider the vector field (3.4), the control law (4.11), and a trajectory $\mathbf{x}(\cdot)$ of $\dot{\mathbf{x}}(t) = \mathbf{f}_{\mathbf{x}}(t, \mathbf{x}(t), \bar{\mathbf{T}}^{cl}(t, \mathbf{x}(t)))$. If $f_k \in \mathcal{P}^0$ for all $k \in \mathcal{M}$, then for all $\mathbf{x}(0) \in (\mathcal{S}^2)^N \times \mathbb{R}^{3N}$, $\lim_{t\to\infty}(B\otimes \mathrm{I})\mathbf{e}(\mathbf{n}(t)) = \mathbf{0}$, $\lim_{t\to\infty} \boldsymbol{\omega}_i(t) = \mathbf{0}$ for $i \in \mathcal{L}$ and $\lim_{t\to\infty} \Pi(\bar{\mathbf{n}}_j)\boldsymbol{\omega}_j(t) = \mathbf{0}$ for $j \in \bar{\mathcal{L}}$; additionally, if $\mathbf{x}(0) \in \Omega^0_{\mathbf{x}} = \{\mathbf{x} \in (\mathcal{S}^2)^N \times \mathbb{R}^{3N} : \exists p \in \mathcal{M}, V(\mathbf{x}) < p d^{\min}\}$, then no more than $p-1$ neighbors are ever diametrically opposed, i.e., $\sup_{t\geq 0} |\{q \in \mathcal{M} : {}_q\mathbf{n}^T(t)_{\bar{q}}\mathbf{n}(t) = -1\}| \leq p-1$.

Proof Notice that if $f_k \in \mathcal{P}^0$ for all $k \in \mathcal{M}$ then $\Omega^{\mathbf{e}}_{\mathbf{n}} = \Omega^D_{\mathbf{n}} = (\mathcal{S}^2)^N$, which is a compact set. Since $\mathbf{e}(\cdot)$ is continuous in $\Omega^{\mathbf{e}}_{\mathbf{n}}$, it follows that $\max_{\mathbf{n}\in\Omega^{\mathbf{e}}_{\mathbf{n}}} \|\mathbf{e}(\mathbf{n})\| < \infty$, and, therefore, $\|\mathbf{e}(\mathbf{n}(\cdot))\|$ is bounded regardless of the trajectory $\mathbf{x}(\cdot)$. To conclude that $\lim_{t\to\infty}(B\otimes \mathrm{I})\mathbf{e}(\mathbf{n}(t)) = \mathbf{0}$, $\lim_{t\to\infty} \boldsymbol{\omega}_i(t) = \mathbf{0}$ for $i \in \mathcal{L}$ and $\lim_{t\to\infty} \Pi(\bar{\mathbf{n}}_j)\boldsymbol{\omega}_j(t) = \mathbf{0}$ for $j \in \bar{\mathcal{L}}$, it suffices to follow the same steps as in the proof of Proposition 4.5. For the final statement in the Proposition, consider $\mathbf{x}(0) \in \Omega^0_{\mathbf{x}} = \{\mathbf{x} \in \Omega_{\mathbf{x}} : \exists p \in \mathcal{M}, V(\mathbf{x}) < p d^{\min}\}$. Since, along a trajectory $\mathbf{x}(\cdot)$, $D(\mathbf{n}(\cdot)) \leq V(\mathbf{x}(\cdot)) \leq V(\mathbf{x}(0)) < p d^{\min}$, it suffices to invoke Proposition 4.4, with $\bar{D} = V(\mathbf{x}(0))$, and the Proposition's conclusion follows. $\square$

Denote $\mathbf{f}^{cl}_{\mathbf{x}}(t, \mathbf{x}) := \mathbf{f}_{\mathbf{x}}(t, \mathbf{x}, \bar{\mathbf{T}}^{cl}(t, \mathbf{x}))$ as the closed-loop vector field. Note then that $\Omega^{\text{eq}}_{\mathbf{x}} = \{\mathbf{x} \in (\mathcal{S}^2)^N \times \mathbb{R}^{3N} : \forall t \geq 0, \mathbf{f}^{cl}_{\mathbf{x}}(t, \mathbf{x}) = \mathbf{0}\}$ provides the set of all equilibrium points, and moreover $\{\mathbf{x} \in (\mathcal{S}^2)^N \times \mathbb{R}^{3N} : (B\otimes \mathrm{I})\mathbf{e}(\mathbf{n}) = \mathbf{0}, \boldsymbol{\omega}_i = \mathbf{0} \text{ for } i \in \mathcal{L}, \Pi(\bar{\mathbf{n}}_j)\boldsymbol{\omega}_j = \mathbf{0} \text{ for } j \in \bar{\mathcal{L}}\} \subseteq \Omega^{\text{eq}}_{\mathbf{x}}$. As such, Propositions 4.5 and 4.6 imply that, under the respective Propositions' conditions, a trajectory $\mathbf{x}(\cdot)$ converges to the set of equilibrium points. Note also that $[(\mathbf{1}_N \otimes \mathbf{n}^\star)^T \cdot]^T \in \Omega^{\text{eq}}_{\mathbf{x}}$ for all $\mathbf{n}^\star \in \mathcal{S}^2$, i.e., all configurations where all agents are synchronized are equilibrium configurations (agents are synchronized and not moving, or agents are synchronized and spinning around their principal axis). Finally, notice that since $\mathbf{e}(\mathbf{Sn}) = \mathbf{e}(\mathbf{n})$ for all $\mathbf{S} \in \{\mathrm{I}_N \otimes \mathcal{R} \in \mathbb{R}^{3N\times 3N} : \mathcal{R} \in \mathcal{SO}(3)\}$ and for all $\mathbf{n} \in \Omega^{\mathbf{e}}_{\mathbf{n}}$, it follows that $\Omega^{\text{eq}}_{\mathbf{x}}$ has *geometric isomerism* [Li and Spong, 2014]; i.e. $[\mathbf{n}^T \cdot]^T \in \Omega^{\text{eq}}_{\mathbf{x}} \Rightarrow [\mathbf{Sn}^T \cdot]^T \in \Omega^{\text{eq}}_{\mathbf{x}}$, which means that for every equilibrium configuration, there exits infinite other equilibria configurations which are the same up to a rotation. In Section 5, for tree graphs, we show that $\Omega^{\text{eq}}_{\mathbf{x}}$ is composed of configurations where agents are either synchronized or diametrically opposed; while in Section 6, for graphs as those discussed in Proposition 4.1, we show that $\Omega^{\text{eq}}_{\mathbf{x}}$ is composed of configurations where agents belong to a common plane. In light of these comments, it follows that Corollary 4.1 provides conditions for when a trajectory is guaranteed to converge to a configuration where all agents are synchronized, and not any other configuration in $\Omega^{\text{eq}}_{\mathbf{x}}$; in particular, if the initial kinetic energy is *too large* with respect to $d^{\min}$, the agents may escape to other equilibria configurations other than synchronized ones.

Remark 4.1 In our framework, where in general $J_i \neq j_i \mathrm{I}$ for some $i \in \mathcal{N}$ and $j_i > 0$, invariance of the closed-loop dynamics to rotations does not hold due to the term $\mathcal{S}(\boldsymbol{\omega}_i) J_i \boldsymbol{\omega}_i$ in (3.3) [Pereira and Dimarogonas, 2016].

5 Tree Graphs

Let us focus first on static tree graphs, for which $\mathcal{N}(B\otimes \mathrm{I}) = \{\mathbf{0}\}$ [Dimarogonas and Johansson, 2009]. In this section, we quantify the domain of attraction for synchronization to be asymptotically reached, i.e., we construct a domain $\Omega^0_{\mathbf{x}}$ such that if $\mathbf{x}(0) \in \Omega^0_{\mathbf{x}}$, then all trajectories of $\dot{\mathbf{x}}(t) = \mathbf{f}_{\mathbf{x}}(t, \mathbf{x}(t), \bar{\mathbf{T}}^{cl}(t, \mathbf{x}(t)))$ (see (3.4) and (4.11)) asymptotically converge to a configuration where all unit vectors are synchronized. Later, we construct another set $\Omega^0_{\mathbf{x}}$, for graphs other than tree graphs, which is smaller in size, and we quantify how much smaller it is.

Theorem 5.1 Consider a static tree network graph, the vector field (3.4), the control law (4.11), and a trajectory $\mathbf{x}(\cdot)$ of $\dot{\mathbf{x}}(t) = \mathbf{f}_{\mathbf{x}}(t, \mathbf{x}(t), \bar{\mathbf{T}}^{cl}(t, \mathbf{x}(t)))$. If $\mathbf{x}(0) \in \Omega^0_{\mathbf{x}} = \{\mathbf{x} \in \Omega^D_{\mathbf{n}} \times \mathbb{R}^{3N} : V(\mathbf{x}) < d^{\min}\}$ then synchronization is asymptotically reached, i.e., $\lim_{t\to\infty}(\mathbf{n}_i(t) - \mathbf{n}_j(t)) = \mathbf{0}$, for all $(i,j) \in \mathcal{N}^2$. If $f_k \in \mathcal{P}^\infty$ for all $k \in \mathcal{M}$, then $d^{\min} = \infty$ and synchronization is asymptotically reached for almost all initial conditions in $(\mathcal{S}^2)^N \times \mathbb{R}^{3N}$.

Proof Under the Theorem's conditions, we can invoke Propositions 4.5 and 4.4 to conclude, respectively, that $\lim_{t\to\infty}(B\otimes \mathrm{I})\mathbf{e}(\mathbf{n}(t)) = \mathbf{0}$ and that two neighbors are never arbitrarily close to a configuration where they are diametrically opposed. Since $\mathcal{N}(B\otimes \mathrm{I}) = \{\mathbf{0}\}$, it follows that $\lim_{t\to\infty}(B\otimes \mathrm{I})\mathbf{e}(\mathbf{n}(t)) = \mathbf{0} \Rightarrow \lim_{t\to\infty} \mathbf{e}(\mathbf{n}(t)) = \mathbf{0}$. As such, and since two neighbors are never arbitrarily close to a configuration where they are diametrically opposed, it follows that all unit vectors converge to one another. For the second part of the Theorem, notice that, if $d^{\min} = \infty$, then $\Omega^0_{\mathbf{x}} = \Omega^D_{\mathbf{n}} \times \mathbb{R}^{3N}$. Since $\Omega^D_{\mathbf{n}} \times \mathbb{R}^{3N} \backslash \{(\mathcal{S}^2)^N \times \mathbb{R}^{3N}\} = \{\mathbf{x} \in (\mathcal{S}^2)^N \times \mathbb{R}^{3N} : {}_k\mathbf{n}^T{}_{\bar{k}}\mathbf{n} \neq -1, \forall f_k \in \mathcal{P}^\infty\}$ is a set of zero measure in the space of all initial conditions, i.e. $(\mathcal{S}^2)^N \times \mathbb{R}^{3N}$, synchronization for almost all initial conditions is guaranteed for $d^{\min} = \infty$. $\square$

Notice that in Theorem 5.1, increasing $d^{\min}$ enlarges the region of stability, and it yields the almost global stability result for $d^{\min} = \infty$. However, a similar result for other graphs, other than tree graphs, is not presented in this manuscript.

Example 5.1 Consider the distance functions $d(\mathbf{n}_1, \mathbf{n}_2) = f(1 - \mathbf{n}_1^T \mathbf{n}_2)$ where $f(s) = a\left(\pi^{-1} \arccos(1-s)\right)^\alpha$, with $a > 0$ and $\alpha \geq 2$. For these, $d^{\max} = a$, $f \in \mathcal{P}^\infty$ and $f \in \mathcal{P}^{\bar{0}}$; also $f \in \mathcal{P}_0$. Suppose $f_k(s) = f(s)$ for all $k \in \mathcal{M}$, and for some a and α. Invoking Corollary 4.1, it follows that if $r := \frac{H(\boldsymbol{\omega}(0))}{a} < 1$ and $\mathbf{n}(0) \in \mathcal{C}\left(\frac{\pi}{2}\left(\frac{1-r}{M}\right)^{\frac{1}{\alpha}}\right)$ then Theorem's 5.1 conclusions follow. Notice that by increasing a convergence for arbitrary initial values of rotational kinetic energy can be guaranteed; on the other hand, by increasing α we can increase the size of the cone where the agents need to initially be contained in (up to $\mathcal{C}\left(\frac{\pi}{2}\right)$). Nevertheless, the domain of attraction in Theorem 5.1 is larger, in the sense that there are initial conditions which do not satisfy the previous conditions, but for which synchronization is still guaranteed.

Theorem 5.2 Consider a static tree network graph, the vector field (3.4), the control law (4.11), and a trajectory $\mathbf{x}(\cdot)$ of $\dot{\mathbf{x}}(t) = \mathbf{f}_{\mathbf{x}}(t, \mathbf{x}(t), \bar{\mathbf{T}}^{cl}(t, \mathbf{x}(t)))$. If $f_k \in \mathcal{P}^0$ for all $k \in \mathcal{M}$, and $\mathbf{x}(0) \in \Omega^0_{\mathbf{x}} = \{\mathbf{x} \in \Omega^D_{\mathbf{n}} \times \mathbb{R}^{3N} : \exists p \in \mathcal{M}, V(\mathbf{x}) < p d^{\min}\}$ then the group of unit vectors converges to a configuration where no more than $p-1$ neighboring unit vectors are diametrically opposed.

Proof Under the Theorem's conditions, Proposition 4.6 can be invoked. Additionally, since $\mathcal{N}(B \otimes \mathrm{I}) = \{\mathbf{0}\}$ in a tree graph, it follows that $\lim_{t\to\infty}(B \otimes \mathrm{I})\mathbf{e}(\mathbf{n}(t)) = \mathbf{0} \Rightarrow \lim_{t\to\infty} \mathbf{e}(\mathbf{n}(t)) = \mathbf{0}$, which implies that all neighbors are either synchronized or diametrically opposed. Since, by Proposition 4.6, there are at most $p-1$ diametrically opposed neighboring unit vectors, it follows that the group of unit vectors converges to a configuration where no more than $p-1$ neighboring unit vectors are diametrically opposed. $\square$

Under Theorem's 5.2 conditions, the group of agents can converge to configurations where one or more pairs of neighbors are diametrically opposed. However, it does not provide any insight on whether these equilibrium configurations are stable or unstable; neither on whether the limits $\lim_{t\to\infty} \mathbf{n}_i(t)$ (for all $i \in \mathcal{N}$) exist. See [Pereira and Dimarogonas, 2016] for some remarks on these topics.

6 Non-Tree Graphs

In this section, we study the equilibria configurations induced by some more general, yet specific, network graphs. Also, we study the local stability properties of the synchronized configuration for arbitrary graphs. We first give the following definition.

Definition 6.1 Given $\mathbf{x}_1, \cdots, \mathbf{x}_N \in \mathbb{R}^3$, we say that $\{\mathbf{x}_i\}_{i\in\{1,\cdots,n\}}$ *belong to a common plane* if there exists a unit vector $\boldsymbol{\nu} \in \mathcal{S}^2$ such that $\Pi(\boldsymbol{\nu})\mathbf{x}_i = \mathbf{x}_i$ for all $i \in \{1, \cdots, n\}$. We say that $\{\mathbf{x}_i\}_{i\in\{1,\cdots,n\}}$ *belong to a common unique plane* if there exists a single pair of unit vectors $(+\boldsymbol{\nu}, -\boldsymbol{\nu})$, with $\boldsymbol{\nu} \in \mathcal{S}^2$, such that $\Pi(\boldsymbol{\nu})\mathbf{x}_i = \mathbf{x}_i$ for all $i \in \{1, \cdots, n\}$

Let us first discuss a property that is exploited later in this section.

Proposition 6.1 Consider $\mathbf{n}_1, \mathbf{n}_2 \in \mathcal{S}^2$. If $\mathcal{S}(\mathbf{n}_1)\mathbf{n}_2 \neq \mathbf{0}$, then $\mathbf{n}_1$ and $\mathbf{n}_2$ belong a common unique plane.

Proof Consider $\boldsymbol{\nu} = \frac{\mathcal{S}(\mathbf{n}_1)\mathbf{n}_2}{\|\mathcal{S}(\mathbf{n}_1)\mathbf{n}_2\|} \in \mathcal{S}^2$, which is well defined since $\mathcal{S}(\mathbf{n}_1)\mathbf{n}_2 \neq \mathbf{0}$. It follows that $\Pi(\boldsymbol{\nu})\mathbf{n}_1 = \mathbf{n}_1$ and that $\Pi(\boldsymbol{\nu})\mathbf{n}_2 = \mathbf{n}_2$, which implies that $\mathbf{n}_1$ and $\mathbf{n}_2$ belong a common plane. Moreover, $\mathbf{n}_1$ and $\mathbf{n}_2$ belong a common unique plane, since $\mathbf{n}_1$ and $\mathbf{n}_2$ span a two dimensional space. $\square$

Proposition 6.2 Consider $\mathbf{n}_1, \ldots, \mathbf{n}_n \in \mathcal{S}^2$, with $|\mathbf{n}_i^T \mathbf{n}_{i+1}| \neq 1$ for all $i = \{1, \cdots, n-1\}$. If $\pm\frac{\mathcal{S}(\mathbf{n}_1)\mathbf{n}_2}{\|\mathcal{S}(\mathbf{n}_1)\mathbf{n}_2\|} = \cdots = \pm\frac{\mathcal{S}(\mathbf{n}_{n-1})\mathbf{n}_n}{\|\mathcal{S}(\mathbf{n}_{n-1})\mathbf{n}_n\|}$, then all unit vectors belong to a common unique plane.

Proof Consider $n = 3$. Since $|\mathbf{n}_1^T \mathbf{n}_2| \neq 1$ and $|\mathbf{n}_2^T \mathbf{n}_3| \neq 1$, it follows that $\|\mathcal{S}(\mathbf{n}_1)\mathbf{n}_2\| \neq 0$ and $\|\mathcal{S}(\mathbf{n}_2)\mathbf{n}_3\| \neq 0$. Additionally, by assumption, $\pm\frac{\mathcal{S}(\mathbf{n}_1)\mathbf{n}_2}{\|\mathcal{S}(\mathbf{n}_1)\mathbf{n}_2\|} = \pm\frac{\mathcal{S}(\mathbf{n}_2)\mathbf{n}_3}{\|\mathcal{S}(\mathbf{n}_2)\mathbf{n}_3\|}$, is satisfied. Consider then $\boldsymbol{\nu} = \frac{\mathcal{S}(\mathbf{n}_1)\mathbf{n}_2}{\|\mathcal{S}(\mathbf{n}_1)\mathbf{n}_2\|} \in \mathcal{S}^2$. It follows immediately that $\Pi(\boldsymbol{\nu})\mathbf{n}_1 = \mathbf{n}_1$ and that $\Pi(\boldsymbol{\nu})\mathbf{n}_2 = \mathbf{n}_2$. It also follows that $\Pi(\boldsymbol{\nu})\mathbf{n}_3 = (\mathrm{I} - \boldsymbol{\nu}\boldsymbol{\nu}^T)\mathbf{n}_3 = \mathbf{n}_3 - \boldsymbol{\nu}(\boldsymbol{\nu}^T\mathbf{n}_3) = \mathbf{n}_3$, where $\boldsymbol{\nu}^T\mathbf{n}_3 = 0$ follows from taking the inner product of $\pm\frac{\mathcal{S}(\mathbf{n}_1)\mathbf{n}_2}{\|\mathcal{S}(\mathbf{n}_1)\mathbf{n}_2\|} = \pm\frac{\mathcal{S}(\mathbf{n}_2)\mathbf{n}_3}{\|\mathcal{S}(\mathbf{n}_2)\mathbf{n}_3\|}$ with $\mathbf{n}_3$. Altogether, it follows that $\mathbf{n}_1$, $\mathbf{n}_2$ and $\mathbf{n}_3$ belong to a common unique plane (see Proposition 6.1). For $n > 3$, it suffices to apply the previous argument $n-2$ times. $\square$

Proposition 6.3 Consider $\mathbf{n}_1, \ldots, \mathbf{n}_n \in \mathcal{S}^2$ and recall (4.2). If $\pm\mathbf{e}_1(\mathbf{n}_1, \mathbf{n}_2) = \cdots = \pm\mathbf{e}_{n-1}(\mathbf{n}_{n-1}, \mathbf{n}_n)$ then all unit vectors belong to a common plane, which is unique if $\pm\mathbf{e}_1(\mathbf{n}_1, \mathbf{n}_2) = \cdots = \pm\mathbf{e}_{n-1}(\mathbf{n}_{n-1}, \mathbf{n}_n) \neq \mathbf{0}$.

Proof If $\pm\mathbf{e}_1(\mathbf{n}_1, \mathbf{n}_2) = \cdots = \pm\mathbf{e}_{n-1}(\mathbf{n}_{n-1}, \mathbf{n}_n) \neq \mathbf{0}$, it suffices to invoke Proposition 6.2. If $\pm\mathbf{e}_1(\mathbf{n}_1, \mathbf{n}_2) = \cdots = \pm\mathbf{e}_{n-1}(\mathbf{n}_{n-1}, \mathbf{n}_n) = \mathbf{0}$, it follows that $\pm\mathbf{n}_1 = \cdots = \pm\mathbf{n}_n$, and thus all unit vectors belong to a common plane. $\square$

Theorem 6.1 Consider the vector field (3.4), the control law (4.11) with $f_k \in \mathcal{P}^0$ for all $k \in \mathcal{M}$, and a trajectory $\mathbf{x}(\cdot)$ of $\dot{\mathbf{x}}(t) = \mathbf{f}_{\mathbf{x}}(t, \mathbf{x}(t), \bar{\mathbf{T}}^{cl}(t, \mathbf{x}(t)))$. If the network graph contains only independent cycles and/or cycles that share only one edge, then all unit vectors belonging

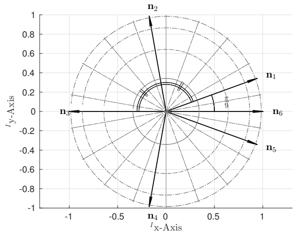

(a) Equilibrium

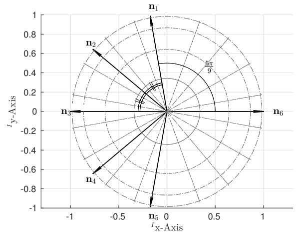

(b) Equilibrium

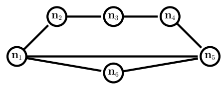

(c) Network graph

Fig. 5. Two equilibrium configurations for group with network graph shown in Fig. 5(c) with two cycles that share only one edge; the equilibria in Fig 5(a) and 5(b) are found with the distance function $f(s) = s$ for all edges.

to each independent cycle converge to a common plane, and all unit vectors belonging to each pair of cycles that share only one edge also converge to a common plane.

Proof (Sketch of Proof) Under the conditions of the Theorem, we can invoke Proposition 4.6, from which it follows that $\lim_{t\to\infty}(B \otimes \mathrm{I})\mathbf{e}(\mathbf{n}(t)) = \mathbf{0}$, and therefore that $\mathbf{e}(\mathbf{n}(\cdot))$ converges to the null space of $B \otimes \mathrm{I}$. Now, consider a graph with only independent cycles and recall Proposition 4.1 (with $n_2 = 0$). Without loss of generality, consider that there is only one independent cycle and that the first $n \geq 3$ edges form that cycle. From Proposition 4.1, it follows that $\mathbf{e}(\mathbf{n}) \in \mathcal{N}(B \otimes \mathrm{I}) \Rightarrow \pm\mathbf{e}_1({}_1\mathbf{n}, {}_{\bar{1}}\mathbf{n}) = \cdots = \pm\mathbf{e}_n({}_n\mathbf{n}, {}_{\bar{n}}\mathbf{n})$. In turn, from Proposition 6.3, it follows that all unit vectors that form the cycle belong to a common plane when $(B \otimes \mathrm{I})\mathbf{e}(\mathbf{n}) = \mathbf{0}$. $\square$

The complete proof of Theorem 6.1 is found in [Pereira and Dimarogonas, 2016] and relies on asserting, with the help of Proposition 4.1, that the only way all edges belong to the null-space of $B \otimes \mathrm{I}$ is by belonging to a common plane. Figure 5 exemplifies the statement in Theorem 6.1, with a network of six agents, with the network graph in Fig. 5(c), and where the distance function is the same for all edges ($f_1(s) = \cdots = f_7(s) = s$). In this scenario, there are two cycles that share only one edge, one cycle composed by the unit vectors $\{\mathbf{n}_1, \mathbf{n}_2, \mathbf{n}_3, \mathbf{n}_4, \mathbf{n}_5\}$, a second cycle composed by the unit vectors $\{\mathbf{n}_1, \mathbf{n}_5, \mathbf{n}_6\}$, and where the shared edge is formed by $\{\mathbf{n}_1, \mathbf{n}_5\}$. There are at least two equilibria configurations (apart from configurations where $\mathbf{n}_i = \pm\mathbf{n}_j$ for some i and j), which are given in Fig. 5(a) and Fig. 5(b), where in both cases all unit vectors belong to a common plane.

Proposition 6.1 focus on equilibria for some general, yet specific, network graphs. However, for arbitrary graphs, we can find equilibria configurations where the unit vectors do not necessarily belong to a common plane [Pereira and Dimarogonas, 2016].

We now present a proposition, which will be useful in guaranteeing local asymptotic stability of incomplete attitude synchronization for arbitrary graphs.

Proposition 6.4 Consider $\mathbf{n} = (\mathbf{n}_1, \cdots, \mathbf{n}_N) \in \bar{\mathcal{C}}(\alpha)$, for some $\alpha \in [0, \frac{\pi}{2})$, and consider also *i)* a connected network graph; *ii)* and that $\mathbf{e}(\mathbf{n}) \in \mathcal{N}(B \otimes \mathrm{I})$, with $\mathbf{e}(\cdot)$ as in (4.3). This takes place iff $\exists \boldsymbol{\nu} \in \mathcal{S}^2 : \mathbf{n} = (\mathbf{1}_N \otimes \boldsymbol{\nu})$.

Proof For the sufficiency statement, it follows that, if $\exists \boldsymbol{\nu} \in \mathcal{S}^2 : \mathbf{n} = (\mathbf{1}_N \otimes \boldsymbol{\nu})$, then all unit vectors are contained in a $\frac{\pi}{2}$-cone, i.e., $\mathbf{n} \in \mathcal{C}(\frac{\pi}{2})$; and, moreover, $\mathbf{e}(\mathbf{1}_N \otimes \boldsymbol{\nu}) = \mathbf{0} \in \mathcal{N}(B \otimes \mathrm{I})$. For the necessity statement, the proof is as follows. For a tree graph, $(B \otimes \mathrm{I})\mathbf{e}(\mathbf{n}) = \mathbf{0} \Leftrightarrow \mathbf{e}(\mathbf{n}) = \mathbf{0}$ follows. This implies that $\mathbf{n}_i = \pm\mathbf{n}_j$ for all $(i, j) \in \mathcal{E}$, but since $\mathbf{n} \in \mathcal{C}(\frac{\pi}{2})$, it follows that $\mathbf{n}_i = \mathbf{n}_j$ for all $(i, j) \in \mathcal{E}$. In a connected graph, this implies that $\mathbf{n}_i = \mathbf{n}_j$ for all $(i, j) \in \mathcal{N} \times \mathcal{N}$, and therefore $\exists \boldsymbol{\nu} \in \mathcal{S}^2 : \mathbf{n} = (\mathbf{1}_N \otimes \boldsymbol{\nu})$. For an arbitrary graph, the null space of $(B \otimes \mathrm{I})$ may be more than $\{\mathbf{0}\}$, i.e., $(B \otimes \mathrm{I})\mathbf{e}(\cdot) = \mathbf{0} \not\Rightarrow \mathbf{e}(\cdot) = \mathbf{0}$. We anticipate the final result by stating that if $\mathbf{n} \in \mathcal{C}(\frac{\pi}{2})$, then $(B \otimes \mathrm{I})\mathbf{e}(\mathbf{n}) = \mathbf{0} \Rightarrow \mathbf{e}(\mathbf{n}) = \mathbf{0}$, in which case we conclude again that $\exists \boldsymbol{\nu} \in \mathcal{S}^2 : \mathbf{n} = (\mathbf{1}_N \otimes \boldsymbol{\nu})$. Consider then an $\mathbf{n} = (\mathbf{n}_1, \cdots, \mathbf{n}_N) \in (\mathcal{S}^2)^N$, such that $(B \otimes \mathrm{I})\mathbf{e}(\mathbf{n}) = \mathbf{0}$. This means that, for every $i \in \mathcal{N}$ ($B_{i:}$ stands for the i^{th} row of B),

$$\mathbf{0} = (B_{i:} \otimes \mathrm{I})\mathbf{e}(\mathbf{n}) \overset{(4.2)}{=} \mathcal{S}(\mathbf{n}_i) \sum_{j \in \mathcal{N}_i} f'_{\kappa(i,j)}(1 - \mathbf{n}_i^T\mathbf{n}_j)\mathbf{n}_j. \quad (6.1)$$

Since $\mathbf{n} \in \bar{\mathcal{C}}(\alpha)$, it follows that there exists a unit vector $\boldsymbol{\mu} \in \mathcal{S}^2$, such that $\boldsymbol{\mu}^T\mathbf{n}_i \geq \cos(\alpha) > 0$ for all $i \in \mathcal{N}$. Taking the inner product of (6.1) with $\mathcal{S}(\mathbf{n}_i)\boldsymbol{\mu}$, it follows that $\boldsymbol{\mu}^T\Pi(\mathbf{n}_i)\sum_{j\in\mathcal{N}_i} f'_{\kappa(i,j)}(1 - \mathbf{n}_i^T\mathbf{n}_j)\mathbf{n}_j = \mathbf{0}$, which can be expanded into

$$\sum\nolimits_{j\in\mathcal{N}_i} f'_{\kappa(i,j)}(1 - \mathbf{n}_i^T\mathbf{n}_j)\left(\boldsymbol{\mu}^T\mathbf{n}_j - (\boldsymbol{\mu}^T\mathbf{n}_i)\mathbf{n}_i^T\mathbf{n}_j\right) = 0 \quad (6.2)$$

Now, consider the set $\mathcal{T} = \{i \in \mathcal{N} : i = \arg\max_{i\in\mathcal{N}}(1 - \boldsymbol{\mu}^T\mathbf{n}_i)\}$, and choose $k \in \mathcal{T}$ (in the end, we show that, in fact, $\mathcal{T} = \mathcal{N}$). Notice that $0 < \cos(\alpha) \leq \boldsymbol{\mu}^T\mathbf{n}_k \leq \boldsymbol{\mu}^T\mathbf{n}_j$ for all $k \in \mathcal{T}$ and all $j \in \mathcal{N}$. As such, it follows from (6.2) with $i = k$ that

$$\begin{aligned} 0 &\leq \cos(\alpha)\sum\nolimits_{j\in\mathcal{N}_k} f'_{\kappa(i,j)}(1 - \mathbf{n}_i^T\mathbf{n}_j)(1 - \mathbf{n}_k^T\mathbf{n}_j) \leq \\ &\leq \sum_{j\in\mathcal{N}_k} f'_{\kappa(i,j)}(1 - \mathbf{n}_i^T\mathbf{n}_j)\left(\boldsymbol{\mu}^T\mathbf{n}_j - (\boldsymbol{\mu}^T\mathbf{n}_k)\mathbf{n}_k^T\mathbf{n}_j\right) = 0. \quad (6.3)\end{aligned}$$

Notice that the lower bound (on the left side of (6.3)) is non-negative and zero if and only if all neighbors of agent k are synchronized with itself (note that $\lim_{s\to 2^-} f'_{\kappa(i,j)}(s)$ may be 0, but since $\mathbf{n} \in \bar{\mathcal{C}}(\alpha)$, $f'_{\kappa(i,j)}(s)|_{s=1-\mathbf{n}_i^T\mathbf{n}_j}$ can only vanish if $s \to 0^+$). As such, it follows from (6.3) that all neighbors of agent k are contained in $\mathcal{T}$, i.e., $\mathcal{N}_k \subset \mathcal{T}$. As such, the same procedure as before can be followed for the neighbors of agent k, to conclude that the neighbors of the neighbors of agent k are all synchronized. In a connected graph, by applying the previous reasoning at most $N - 1$ times, it follows that all unit vectors are synchronized, or, equivalently, that $\exists \boldsymbol{\nu} \in \mathcal{S}^2 : \mathbf{n} = (\mathbf{1}_N \otimes \boldsymbol{\nu})$. $\square$

Proposition 6.4 has the following interpretation. Recall that $\{\mathbf{x} \in (\mathcal{S}^2)^N \times \mathbb{R}^{3N} : (B \otimes \mathrm{I})\mathbf{e}(\mathbf{n}) = \mathbf{0}, \boldsymbol{\omega}_i = \mathbf{0}$ for $i \in \mathcal{L}, \Pi(\bar{\mathbf{n}}_j)\boldsymbol{\omega}_j = \mathbf{0}$ for $j \in \bar{\mathcal{L}}\} \subseteq \Omega_{\mathbf{x}}^{\text{eq}}$, where $\Omega_{\mathbf{x}}^{\text{eq}}$ is the set of equilibrium points. For example, we have seen that, for specific graphs, all equilibrium configurations are such that all unit vectors belong to a common plane (see Theorem 6.1), as illustrated in Fig. 5. However, if we can guarantee that along a trajectory $\mathbf{x}(\cdot)$ of $\dot{\mathbf{x}}(t) = \mathbf{f}_{\mathbf{x}}(t, \mathbf{x}(t), \bar{\mathbf{T}}^{cl}(t, \mathbf{x}(t)))$, $\exists \alpha \in [0, \frac{\pi}{2}) : \mathbf{n}(t) \in \bar{\mathcal{C}}(\alpha), \forall t \geq 0$, i.e., if we can guarantee that all unit vectors remain in an closed α-cone smaller than an open $\frac{\pi}{2}$-cone, then we can invoke Proposition 6.4 to conclude that $\lim_{t\to\infty}(B \otimes \mathrm{I})\mathbf{e}(\mathbf{n}(t)) = \mathbf{0} \Rightarrow \lim_{t\to\infty}(\mathbf{n}_i(t) - \mathbf{n}_j(t)) = \mathbf{0} \forall i, j \in \mathcal{N}$; i.e., that convergence of $\mathbf{e}(\mathbf{n}(\cdot))$ to the null space of $B \otimes \mathrm{I}$ implies synchronization of the agents.

This motivates us to introduce a distance $d^\star > 0$, which is useful in guaranteeing that, along a trajectory $\mathbf{x}(\cdot)$, $\exists \alpha \in [0, \frac{\pi}{2}) : \mathbf{n}(t) \in \bar{\mathcal{C}}(\alpha), \forall t \geq 0$. Consider then

$$d^\star = \min_{k \in \mathcal{M}} f_k\left(1 - \cos\left(\frac{\pi}{3}\frac{1}{N-1}\right)\right) < d^{\min}, \qquad (6.4)$$

which satisfies $f_k^{-1}(d^\star) \leq 1 - \cos\left(\frac{\pi}{3}\frac{1}{N-1}\right)$ for all $k \in \mathcal{M}$. Notice that $d^\star < d^{\min}$, since $d^{\min} = \min_{k\in\mathcal{M}} \lim_{s\to 2^-} f_k(s)$, since $1 - \cos(\frac{\pi}{3}\frac{1}{N-1}) < 2$ for all $N \geq 2$, and since all $f_k(\cdot)$ are increasing functions in $(0, 2)$. As shown next, if $D(\mathbf{n}(0)) < d^\star$ (and $H(\boldsymbol{\omega}(0) = 0)$, then the network of unit vectors is forever contained in a closed α-cone, for some $\alpha \in [0, \frac{\pi}{2})$.

Theorem 6.2 Consider an arbitrary connected network graph, the vector field (3.4), the control law (4.11), and a trajectory $\mathbf{x}(\cdot)$ of $\dot{\mathbf{x}}(t) = \mathbf{f}_{\mathbf{x}}(t, \mathbf{x}(t), \bar{\mathbf{T}}^{cl}(t, \mathbf{x}(t)))$ If $\mathbf{x}(0) \in \Omega_{\mathbf{x}}^0 = \{\mathbf{x} \in \Omega_{\mathbf{n}}^D \times \mathbb{R}^{3N} : V(\mathbf{x}) < d^\star\}$ then synchronization is asymptotically reached, i.e., $\lim_{t\to\infty}(\mathbf{n}_i(t) - \mathbf{n}_j(t)) = \mathbf{0}$, for all $i, j \in \mathcal{N}$. Moreover, all implications of Proposition 4.5 also follow.

Proof Since $d^\star < d^{\min}$, we can invoke Proposition 4.5, and infer that $\lim_{t\to\infty}(B \otimes \mathrm{I})\mathbf{e}(\mathbf{n}(t)) = \mathbf{0}$ (as well as all other implications stated in the Proposition). Since $\dot{V}(\mathbf{x}(\cdot)) \leq 0$, it follows that $f_k(1 - {}_k\mathbf{n}^T(\cdot)_{\bar{k}}\mathbf{n}(\cdot)) \leq D(\mathbf{n}(\cdot)) \leq V(\mathbf{x}(\cdot)) \leq V(\mathbf{x}(0)) < d^\star$, for all $k \in \mathcal{M}$. In turn, this implies that $\theta({}_k\mathbf{n}(\cdot), {}_{\bar{k}}\mathbf{n}(\cdot)) \leq \arccos(1 - f_k^{-1}(d^\star)) < \frac{\pi}{3}\frac{1}{N-1}$, for all $k \in \mathcal{M}$. Since the angular displacement between any two unit vectors $\mathbf{n}_i$ and $\mathbf{n}_j$ in a connected graph satisfies $\theta(\mathbf{n}_i(\cdot), \mathbf{n}_j(\cdot)) \leq (N-1)\max_{k\in\mathcal{M}} \theta({}_k\mathbf{n}(\cdot), {}_{\bar{k}}\mathbf{n}(\cdot))$, it follows that $\sup_{t\geq 0} \theta(\mathbf{n}_i(t), \mathbf{n}_j(t)) < \frac{\pi}{3}$ for all $i, j \in \mathcal{N}$. As such, it follows from Proposition 4.3 that $\mathbf{n}(\cdot) \in \bar{\mathcal{C}}(\frac{3}{2}\sup_{t\geq 0}\theta(\mathbf{n}_i(t), \mathbf{n}_j(t)))$, where $\frac{3}{2}\sup_{t\geq 0}\theta(\mathbf{n}_i(t), \mathbf{n}_j(t)) < \frac{\pi}{2}$. Finally, we invoke Proposition 6.4, which implies that $\lim_{t\to\infty}(B \otimes \mathrm{I})\mathbf{e}(\mathbf{n}(t)) = \mathbf{0} \Rightarrow \lim_{t\to\infty}(\mathbf{n}_i(t) - \mathbf{n}_j(t)) = \mathbf{0}$ for all $i, j \in \mathcal{N}$. □

Let us provide a corollary to Theorem 6.2, with an easier to visualize region of attraction.

Corollary 6.1 Theorem 6.2 holds if $r := \frac{H(\boldsymbol{\omega}(0))}{d^{\min}} < 1$ and if $\mathbf{n}(0) \in \mathcal{C}\left(\frac{1}{2}\arccos\left(1 - \min_{k\in\mathcal{M}} f_k^{-1}\left(\frac{d^\star}{M}(1-r)\right)\right)\right)$, with $d^\star$ as in (6.4).

For proving Corollary 6.1 it suffices to check that if its conditions are satisfied, then $V(\mathbf{x}(0)) < d^\star$.

Remark 6.1 Comparing Theorems 5.1 and 6.2, it follows that the region of attraction in Theorem 5.1 is larger than that in Theorem 6.2. Loosely speaking, the region of attraction in Theorem 5.1 is $\frac{d^{\min}}{d^\star} > 1$ times larger than the region of attraction in Theorem 6.2. This difference comes from the network graph topology, and in fact, a tree network graph provides stronger results.

Theorems 5.1 and 6.2 provide asymptotic results, such as $\lim_{t\to\infty}\mathbf{e}(\mathbf{n}(t)) = \mathbf{0}$. [Pereira and Dimarogonas, 2016] provides some insight on exponential convergence to 0.

7 Simulations

We now present simulations that illustrate some of the results presented previously. For the simulations, we have a group of ten agents, whose network graph is that presented in Fig. 6(e). The moments of inertia were generated by adding a random symmetric matrix (with entries in $[-1, 1]$) to the identity matrix. For the initial conditions, we have chosen $\boldsymbol{\omega}(0) = \mathbf{0}$ and we have randomly generated one set of 10 rotation matrices. For the axes to be synchronized, we have that $\bar{\mathbf{n}}_i$ is the principal axis of J_i, with largest eigenvalue, for $i = \{1, 2, 3, 4, 5\}$, and that $\bar{\mathbf{n}}_i = [1\,0\,0]^T$ for $i = \{6, 7, 8, 9, 10\}$. Therefore, we apply the control law (4.11), with $\bar{\mathcal{L}} = \{1, 2, 3, 4, 5\}$ and $\mathcal{L} = \{6, 7, 8, 9, 10\}$. For the edge 1, we have chosen $f_1(s) = 10\tan^2(0.5\arccos(1-s))$. For the other edges, we have chosen $f_k(s) = 5s$, for $k = \mathcal{M}\backslash\{1\}$. Notice that we have chosen a distance function (for edge 1) that grows unbounded when two unit vectors are diametrically opposed. As such, it follows that agents 1 and 6 will never be diametrically opposed, under the condition that they are not initially diametrically opposed. We have also chosen $\boldsymbol{\sigma}(\mathbf{x}) = k\frac{\sigma_x \mathbf{x}}{\sqrt{\sigma_x^2 + \mathbf{x}^T\mathbf{x}}}$ with $k = 10$ and $\sigma_x = 1$. For this choice, we find that $\sigma^{\max} = k\sigma_x = 10$. As such, for all agents, except 1 and 6, an upper bound on the norm of their torque is given by $\sigma^{\max} + 2 \cdot 5 = 20$ (the factor 2 relates to the fact that all agents, except 1 and 6, have two neighbors, and the factor 5 comes from $f_k(s) = 5s \Rightarrow f_k'(s) = 5$). For agents 1 and 6, no upper bound can be found (more precisely, a bound can be found, but it depends on the initial conditions). Given these choices, it follows from Corollary 6.1 that if $\mathbf{n}(0) \in \mathcal{C}(\approx 1^\circ)$ then synchronization is guaranteed. We emphasize, nonetheless, that Corollary 6.1 provides conservative conditions for synchronization to be achieved, and the domain of attraction is in fact larger. We also emphasize that, for tree graphs, the domain of attraction is considerably larger: for example, if we removed the edges between agents 1 and 2, and between agents 6 and 7, we would obtain a tree graph, and Corollary 4.1 would read as $\mathbf{n}(0) \in \mathcal{C}(\approx 18^\circ)$. Finally, we emphasize that we can increase the size of the cones in Corollaries 4.1 and 6.1, by choosing different distance functions, as exemplified in Example 5.1.

Figure 6 is composed of two simulations: one simulation where the control law is that in (4.11) and another where the control law in (4.11) is corrupted by noise (namely, for each agent $i \in \mathcal{N}$, $\mathbf{T}_i(t) = \bar{\mathbf{T}}_i^{cl}(t, \mathbf{x}(t)) + 0.1\lambda_i[0\,0\,1]^T$, where λ_i corresponds to the largest eigenvalue of J_i). The trajectories of the unit vectors for the described conditions are presented in Figs. 6(a)–6(b) ($\mathcal{R}_i(0)\bar{\mathbf{n}}_i$ marked with a circle and $\mathcal{R}_i(30)\bar{\mathbf{n}}_i$ marked with a cross, for all $i \in \mathcal{N}$). Notice that despite not satisfying conditions of Theorem 6.2 (the unit vectors are not always in a $\frac{\pi}{2}$ cone), incomplete attitude synchronization is still achieved. This can be verified in Figs. 6(c)-6(d), which present the angular error between neighboring agents. In Figs. 6(a) and 6(b), the control laws are different between agents 1–5 and 6–10. The former perform synchronization of principal axes, by applying the constrained control law (4.10); while the later perform synchronization of their first axes, i.e., $\bar{\mathbf{n}}_i = [1\,0\,0]^T$, by applying the control law (4.6). In Fig. 6(d), for which the control laws were corrupted by noise, perfect synchronization is not asymptotically achieved. Instead, the unit vectors converge to a configuration where they remain close to each other (error of $\approx 5°$ between neighbors). As such, these simulations suggest that the chosen control laws provide a certain level of robustness against constant disturbances. Further simulation examples are found in found in [Pereira and Dimarogonas, 2016].

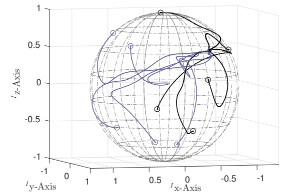
(a) Trajectories w/o noise

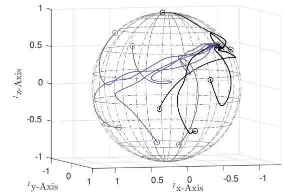
(b) Trajectories with noise

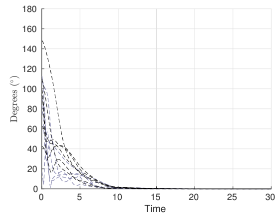
(c) Error angle between neighbors without noise

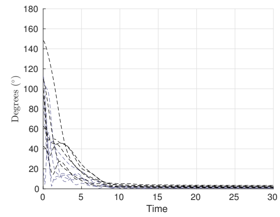
(d) Error angle between neighbors with noise

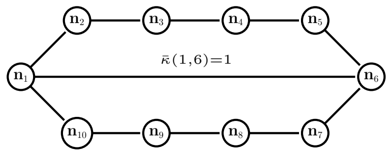

(e) Graph with 10 agents, where edge 1 is formed by agents 1 and 6

Fig. 6. Synchronization in network of 10 unit vectors with and without noise, where blue agents perform synchronization of principal axes and black agents synchronization of their first axes (i.e., $\bar{\mathbf{n}}_i = [1\,0\,0]^T$).

8 Conclusions

In this paper, we proposed a distributed control strategy that guarantees attitude synchronization of unit vectors, representing a specific body direction of a rigid body. The proposed torque control laws depend on distance functions in $\mathcal{S}^2$, and we provide conditions on these distance functions that guarantee that *i)* a synchronized network is locally asymptotically stable in an arbitrary connected undirected network graph; *ii)* a synchronized network is asymptotically achieved for almost all initial conditions in a tree network graph. Also,the proposed control laws can be implemented by each individual rigid body in the absence of a global common orientation frame, i.e., by using only local information. Additionally, if the direction to be synchronized is a principal axis of the rigid body, we proposed a control law that only requires torque in the plane orthogonal to the principal axis. We also studied the equilibria configurations that come with certain types of network graphs.

References

A.K. Bondhus, K.Y. Pettersen, and J.T. Gravdahl. Leader/follower synchronization of satellite attitude without angular velocity measurements. In *IEEE Conference on Decision and Control and European Control Conference*, pages 7270–7277, 2005.

H. Cai and J. Huang. The leader-following attitude control of multiple rigid spacecraft systems. *Automatica*, 50(4):1109–1115, 2014.

S.J Chung, U. Ahsun, and J.J. Slotine. Application of synchronization to formation flying spacecraft: Lagrangian approach. *Journal of Guidance, Control, and Dynamics*, 32(2):512–526, 2009.

S.J. Chung, S. Bandyopadhyay, I. Chang, and F. Hadaegh. Phase synchronization control of complex networks of lagrangian systems on adaptive digraphs. *Automatica*, 49(5):1148–1161, 2013.

D.V. Dimarogonas and K.H. Johansson. Further results on the stability of distance-based multi-robot formations. In *IEEE American Control Conference*, pages 2972–2977, 2009.

D.V. Dimarogonas, P. Tsiotras, and K. Kyriakopoulos. Leader–follower cooperative attitude control of multiple rigid bodies. *Systems & Control Letters*, 58(6): 429–435, 2009.

F. Dörfler and F. Bullo. Synchronization in complex networks of phase oscillators: A survey. *Automatica*, 50(6):1539–1564, 2014.

Ch.D. Godsil, G. Royle, and C.D. Godsil. *Algebraic graph theory*, volume 207. Springer New York, 2001.

S. Guattery and G.L. Miller. Graph embeddings and laplacian eigenvalues. *SIAM Journal on Matrix Analysis and Applications*, 21(3):703–723, 2000.

T.R. Krogstad and J.T. Gravdahl. Coordinated attitude control of satellites in formation. In *Group Coordination and Cooperative Control*, pages 153–170. Springer, 2006.

J.R. Lawton and R.W. Beard. Synchronized multiple spacecraft rotations. *Automatica*, 38(8):1359–1364, 2002.

N.E. Leonard, D.A. Paley, F. Lekien, R. Sepulchre, D.M. Fratantoni, and R.E. Davis. Collective motion, sensor networks, and ocean sampling. *Proceedings of the IEEE*, 95(1):48–74, Jan 2007.

W. Li and M.W. Spong. Unified cooperative control of multiple agents on a sphere for different spherical patterns. *IEEE Transactions on Automatic Control*, 59(5):1283–1289, 2014.

D. Liberzon. *Switching in systems and control*. Springer, 2003.

C.G. Mayhew, R.G. Sanfelice, J. Sheng, M. Arcak, and A.R. Teel. Quaternion-based hybrid feedback for robust global attitude synchronization. *IEEE Transactions on Automatic Control*, 57(8):2122–2127, Aug 2012.

N. Moshtagh and A. Jadbabaie. Distributed geodesic control laws for flocking of nonholonomic agents. *IEEE Transactions on Automatic Control*, 52(4):681–686, 2007.

S. Nair and N. Leonard. Stable synchronization of rigid body networks. *Networks and Heterogeneous Media*, 2(4):597, 2007.

R. Olfati-Saber. Swarms on sphere: A programmable swarm with synchronous behaviors like oscillator networks. In *IEEE Conference on Decision and Control*, pages 5060–5066, 2006.

D. Paley. Stabilization of collective motion on a sphere. *Automatica*, 45(1):212–216, 2009.

P. Pereira and D.V. Dimarogonas. Family of controllers for attitude synchronization in $\mathcal{S}^2$. In *IEEE Conference on Decision and Control*, 2015.

P. Pereira and D.V. Dimarogonas. Family of controllers for attitude synchronization on the sphere. *arXiv*, 2016. URL `http://arxiv.org/pdf/1503.06326v5.pdf`.

A. Sarlette, S.E. Tuna, V. Blondel, and R. Sepulchre. Global synchronization on the circle. In *Proceedings of the 17th IFAC world congress*, pages 9045–9050, 2008.

A. Sarlette, R. Sepulchre, and N.E. Leonard. Autonomous rigid body attitude synchronization. *Automatica*, 45(2):572–577, 2009.

J. Slotine and W. Li. *Applied nonlinear control*, volume 199. Prentice-Hall Englewood Cliffs, NJ, 1991.

W. Song, J. Thunberg, X. Hu, and Y. Hong. Distributed high-gain attitude synchronization using rotation vectors. *Journal of Systems Science and Complexity*, 28 (2):289–304, 2015.

J. Thunberg, W. Song, E. Montijano, Y. Hong, and X. Hu. Distributed attitude synchronization control of multi-agent systems with switching topologies. *Automatica*, 50(3):832–840, 2014.

R. Tron, B. Afsari, and R. Vidal. Intrinsic consensus on SO(3) with almost-global convergence. In *IEEE Conference on Decision and Control*, pages 2052–2058, 2012.